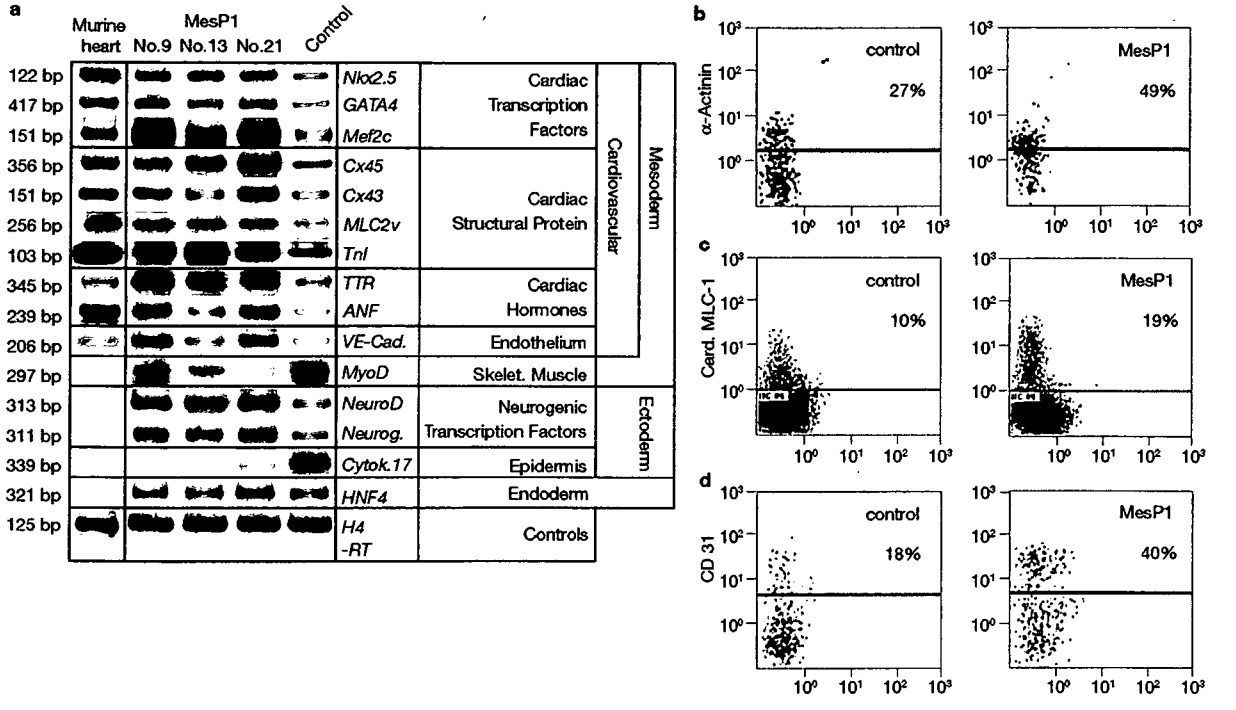

Figure 4 Increased expression of cardiovascular markers in MesP1-overexpressing ES cells. RT-PCR for mesodermal markers at day 6 of differentiation shows an increase in mRNA expression for cardiac markers Nkx 2.5, GATA 4, Mef2c, connexin 45, connexin 43, MLC2v, Tnl, TTR and ANF in three independent *MesP1–IRES–EGFP* clones. In the same clones, mRNA for the endothelial marker VE-Cadherin was increased, whereas the skeletal muscle differentiation marker MyoD was decreased. In the ectodermal lineage *NeuroD* and *Neurogenin* mRNAs were increased, associated with decreased Cytokeratin17 expression. The endodermal marker HNF4 seemed to be unaffected. Full scans of key markers are shown in Supplementary Information, Fig. S6. (**b**) FACS analysis for α-actinin at day 18 of differentiation. Cells expressing α-actinin were increased 1.8-fold in MesP1 clones, compared with control transfected cells. (**c**) FACS analysis for cardiac MLC-1 at day 18 of differentiation. Cells expressing cardiac MLC-1 were increased 1,9-fold in MesP1 clones, compared with control transfected cells. (**d**) FACS analysis for CD31 (PECAM) at day 6 of differentiation. Cells expressing CD31 were increased 2-fold in MesP1 clones, compared with control transfected cells.

after this time-point, the increased cardiovascular differentiation in MesP1-overexpressing clones was confirmed by increases (approximately three-fold) in the Flk1-positive populations (Supplementary Information, Fig. S3). These data suggest that MesP1-based cardiogenesis depends on initial general mesoderm formation[18].

The results in Fig. 5d confirm that the cardiogenic effect of MesP1 is mediated by upregulation of the Wnt inhibitor Dkk-1. To verify our observations, reverse experiments were performed using stably expressed shRNA to knockdown endogenous MesP1. In two independent clones showing reduced MesP1 expression, this approach was accompanied by downregulation of *Dkk-1*, *Nkx2.5* and *GATA-4* mRNA expression (Fig. 5e). To extend the loss of function approach from ES cells to an *in vivo* setting, we performed whole-mount *in situ* hybridization with late gastrulae using wild-type and *MesP1*$^{-/-}$;*MesP2*$^{-/-}$ double knockout embryos[19]. In these embryos the absence of MesP expression led to loss of *Dkk-1* mRNA, specifically in the cardio-cranial mesoderm, caused by either silencing of Dkk-1 transcription or loss of these cells (Fig. 5f). Therefore, Dkk-1 expression in the anterior cardio-cranial mesoderm indeed is dependent on MesP function, whereas Dkk-1 expression in the anterior visceral endoderm and at the base of the allantois is MesP-independent.

To determine whether MesP1 is indeed a transcriptional activator, we performed luciferase assays using our mouse ES-cell lines. Each of the two MesP1 binding-site motifs derived from the *hDkk-1* promoter produced a six- to eight-fold increase in luciferase activity in MesP1-overexpressing cells (Fig. 5g). These results demonstrate that MesP1 acts as a transcriptional activator at the sites identified by ChIP-analysis. These findings were confirmed by *in vivo* experiments, where *hMesP1* mRNA or *hMesP1* expression plasmids were injected into the animal pole of two-cell *Xenopus* embryos, which were then subjected to quantitative RT-PCR analysis for *Dkk-1* mRNA at Nieuwkoop-Faber Stage 14 (Supplementary Information, Fig. S5B). Similarly, injections targeting the mesendoderm of four-cell *Xenopus* embryos showed increased *Dkk-1* mRNA levels (data not shown).

Recently, it has been shown that in *Xenopus*, Wnt antagonists stimulate cardiogenesis non-cell-autonomously, up to several cells away from those in which canonical Wnt/β-catenin signalling is blocked, indicative of an indirect role in heart induction. Dkk-1, which is found in defined mesodermal lineages, including the heart, and other inhibitors of the canonical Wnt pathway, induce Hex expression in endoderm underlying the presumptive cardiac mesoderm. Loss of Hex blocks endogenous cardiogenesis and ectopic heart induction by Dkk-1, whereas ectopic Hex induces expression of cardiac markers non-cell-autonomously[20]. Thus, to initiate cardiogenesis, Wnt antagonists act on endoderm to upregulate Hex, which, in turn, has been suggested to control the production of endoderm-derived, diffusible heart-inducing factors[18,20]. Our observation of a marked increase of *Hex* mRNA in MesP1-overexpressing ES

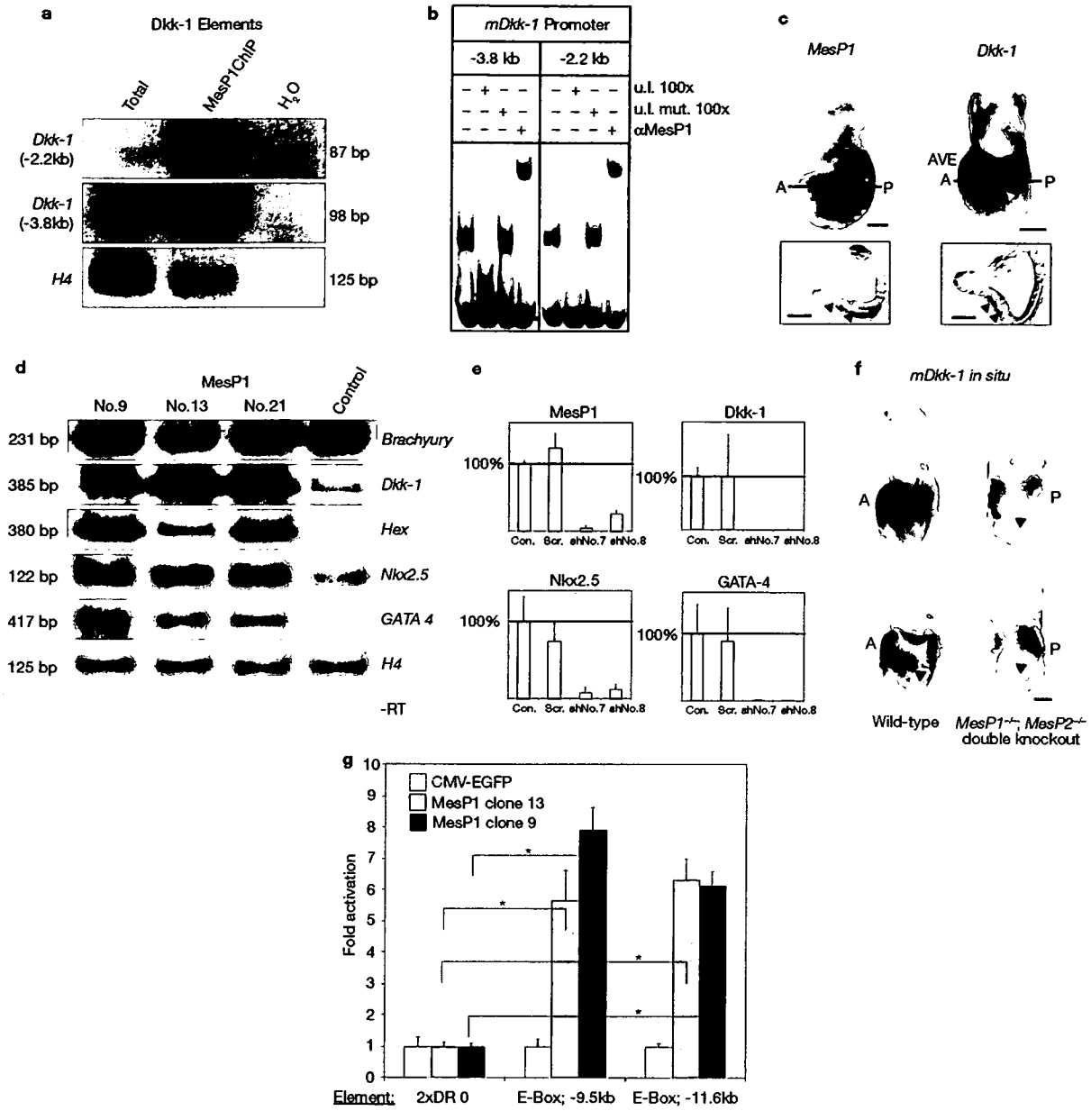

Figure 5 MesP1 enhances cardiovascular differentiation via Dkk-1 mediated blockage of Wnt-signalling. (**a**) PCRs from immunoprecipitated and total input DNA. Two *Dkk-1* promoter-derived PCR-fragments containing bHLH responsive elements were enriched. (**b**) EMSAs using nuclear ES cell extract and the isolated bHLH responsive elements. Lanes 1, 5: specific shift; lanes 2, 6: competition with 100× excess of unlabelled specific probe; lanes 3, 7: competition with 100× excess of unlabelled non-specific probe; lanes 4, 8: supershift. (**c**) Whole-mount samples from *in situ* hybridization of late gastrulae and cross-sections at the indicated level: *MesP1* and *Dkk-1* mRNAs were co-expressed in cardio-cranial mesoderm precursors. Left upper panel: MesP1 expression at E7.5 in mesoderm precursors migrating laterally from the primitive streak to give rise to cardio-cranial mesoderm. MesP1 was also expressed at the base of the allantois (*). Right upper panel: Dkk-1 expression in the anterior visceral endoderm (AVE), the anterior cardio-cranial mesoderm (arrowhead) and the base of the allantois. Sections show *MesP1*-mRNA (left lower panel) in posterior and lateral mesoderm, giving rise to cardio-cranial mesoderm. Right lower panel: Dkk-1 expression in lateral and anterior cardio-cranial mesoderm. Arrowheads: overlapping domains of MesP1 and Dkk-1. Scale bars are 150 μm. (**d**) RT-PCR from MesP1-ES cells (day 3 of differentiation): an increase of mRNA expression for GATA4 and Nkx2.5 but not brachyury was observed in three independent clones. Similarly, mRNAs for the Wnt inhibitor Dkk-1 and Hex were enhanced. Full scans shown in Supplementary Information, Fig. S6. (**e**) Knockdown of endogenous *MesP1* in ES cells using stably expressed shRNA caused reductions in *Dkk-1*, *Nkx2.5* and *GATA-4* mRNA levels (data are mean ± s. d., $n = 4$). (**f**) *In situ* hybridization of late gastrulae for Dkk-1 using wild-type (left) and *MesP1*$^{-/-}$;*MesP2*$^{-/-}$ double knockouts (right): in the knockouts, *Dkk-1* mRNA was specifically lost in the cardio-cranial mesoderm (arrowheads). Scale bar is 150 μm. (**g**) Luciferase assays using control and MesP1-overexpressing ES-cells. Each of the two conserved MesP1-binding sites (E-Box-9.5 kb; E-Box-11.6 kb) was sufficient to enhance luciferase expression 6–8 fold in hMesP1-overexpressing cells versus control ES cells. A control reporter gene containing a bHLH-half-site motif (2× DR 0) was not activated by MesP1 (data are mean ± s. d., $n = 5$, $^*P < 0.0025$).

cells at day 3 of differentiation, leading to high levels of the cardiogenic markers Nkx2.5 and GATA-4, supports these findings (Fig. 5d). On the other hand, it was recently demonstrated that during the period of MesP1 expression, cardiogenic cells themselves are susceptible to Wnt-signalling, confirming that a precise amount and/or timing of Wnt/β-catenin signalling is required for formation of a proper heart tube[21].

In contrast to the requirement for inhibition of canonical Wnt-signalling at the onset of cardiogenesis, canonical Wnt-signalling seems to be required for the expansion and maturation of primary and secondary heart-field-derived cardiomyocytes during further development of the vertebrate heart[22,23]. This is reflected *in vivo* by Wnt8a expression from day 8.5 *post conceptionem* in mouse myocardium of the common ventricular and atrial chambers[24]. Our observation of a decrease in *Dkk-1* mRNA below detection levels in control as well as MesP1-overexpressing ES cells at day 6 of differentiation supports these findings (not shown). In addition, the reduction of *Dkk-1* mRNA to control levels correlates with the 'shut-off' in MesP1 overexpression caused by silencing of the CMV promoter described above (Supplementary Information, Fig. S1).

On the basis of our results, we suggest that MesP1 has a key role during the earliest time points of cardiovascular determination in the lateral plate mesoderm (Supplementary Information, Fig. S5C). This function seems to be highly conserved among chordates[1,2,7–9]. However, in contrast to our experimental conditions, ectopic heart formation in *Ciona* requires a constitutively active form of Cs-MesP[9]. Aside from MesP1 overexpression, an induction of vertebrate myocardial tissue has only been achieved by overexpression of GATA-5 in Zebrafish[25].

It will therefore be of great interest to identify additional direct target genes of MesP1 and factors regulating MesP1 expression. This knowledge will be required to increase the yield of human cardiovascular cells derived from ES cells for future cell therapy and tissue engineering. It will also be of great interest to transfer this approach to various subpopulations of human adult stem cells, whose cardiac transdifferentiation potential has not yet been proven. Manipulation of these cells by overexpression of MesP1 or other factors may help to overcome the hurdles existing for cardiovascular differentiation of adult stem cells in their native state.

METHODS

Plasmid construction. Human full-length *MesP1* cDNA was amplified from human heart cDNA by proofreading PCR using Pfu-Polymerase (Stratagene) and cloned in pCR-XL-Topo (Invitrogen). Subsequently, the cloned PCR fragment was subcloned into the pIRES-EGFP-2 vector (Clontech) using SacI and PstI. After sequencing, this vector was used for electroporation of GSES cells and subsequent selection of stable clones. pEGFP-N1 served as a control transfection plasmid in non-MesP1-overexpressing cells.

***Xenopus* injections.** *Xenopus* embryos used for *in situ* hybridizations or movie documentations were injected with *MesP1* plasmid DNA (100 pg) at the two-cell stage into one blastomere, according to standard protocols[26]. For these experiments, a Globin 5′UTR cassette[27] had been introduced upstream of the *MesP1* cDNA to stabilize the mRNA in the *Xenopus* embryos. For quantitative RT-PCR, embryos used were injected with either *MesP1* mRNA (4 × 60 pg) or *MesP1* plasmid DNA (4 × 60 pg and 4 × 120 pg).

ES cell culture. Electroporation and isolation of stable clones using the mouse ES cell line GSES were performed according to standard protocols, with minor modifications[28]. Non-linearized vector (5 μg) was used for electroporation (240V/500 μF) of GSES cells (5 × 10^6). Transgenic ES cells were grown in high-glucose Dulbecco's modified Eagle medium (DMEM) supplemented with 10% heat-inactivated ES-qualified fetal calf serum (FCS), 2 mM L-glutamine, 50 units ml^{-1} penicillin, 50 μg ml^{-1} streptomycin, 1× non-essential amino acids, 0.4 mg ml^{-1} geneticin (G418) (Gibco), and 0.1 mM β-mercaptoethanol (Sigma). The cells were maintained in an undifferentiated state under feeder-free conditions by addition of 1000 units ml^{-1} purified recombinant mouse LIF (ESGRO, Life Technologies). Cells were maintained at 37 °C in a humidified atmosphere of 5% CO_2/95% air. Monolayers were passaged by trypsinization at confluence (70–80%). For FACS, differentiated cells were dissociated using PBS containing 5 mM EDTA, as described below. *In vitro* differentiation was initiated as follows: GSES cells were collected with 0.25% trypsin-EDTA and dissociated cells were transferred to bacteriological dishes at a density of 2 × 10^5 ES cells ml^{-1} in Iscove's modified Eagle's medium (IMEM, Sigma) supplemented with 10% heat-inactivated FCS, 2 mM L-glutamine, 50 units ml^{-1} penicillin, 50 μg ml^{-1} streptomycin, 1× non-essential amino acids (Life Technologies) and 450 μM α-monothioglycerol (Sigma). After 2 days, EBs were transferred to new medium. At day 6, EBs of similar size were plated on gelatin-coated tissue culture dishes. The growth medium for the attached differentiation cultures was changed every day.

Western blotting. A peptide antibody specific for amino acids 55–69 of human MesP1 was raised in rabbit and affinity purified. Western blotting was performed according to standard protocols, as previously described[26].

RT-PCR. Semi-quantitative RT-PCR incorporating ^{32}P was performed as described previously[6]. The PCR fragments corresponded to base pairs (bp) 64–189 of *H4*, bp 641–1058 of *GATA4*, bp 1332–1454 of *Nkx2.5*, bp 580–810 of *brachyury*, bp 593–831 of *ANF*, bp 76–226 of *connexin 43*, bp 3–358 of *connexin 45*, bp 1326–1476 of *Mef2c*, bp 5–349 of *TTR*, bp 511–613 of *TnI*, bp 5–260 of *MLC2v*, bp 65–270 of *VE-cadherin*, bp 4–300 of *MyoD*, bp 81–393 of *Neuro D*, bp 315–625 of neurogenin, bp 17–356 of *Cytokeratin 17*, bp 66–386 of *HNF-4*, bp 409–721 of *Oct4*, bp 5–271 of *Nanog*, bp 165–419 of *Rex-1*, bp 50–435 of *Dkk-1* and bp99–478 of *Hex*. The annealing temperature was 57 °C for all primer pairs using 25–32 cycles.

Flow cytometry. For FACS analysis to detect EGFP expression, cells were dissociated in PBS containing 5 mM EDTA for 15 min at 37 °C after washing them twice in PBS without calcium. Subsequently, the cells were centrifuged at 900*g* for 3 min in an Eppendorf centrifuge and resuspended in 100 μl ice-cold PBS containing 2% bovine serum albumin. FACS analysis for EGFP expression was performed immediately after this procedure. For FACS analysis of CD31/PECAM-expressing cells, the protocol included an incubation in PE-conjugated αCD31-antibodies (BD Pharmingen), according to the manufacturer's protocol, before measuring. PE-conjugated $IgG_{2a}κ$ served as isotype controls. FACS analysis for α-actinin was performed as described previously [11], using the primary antibody EA53 (Sigma-Aldrich) and a PE-conjugated secondary antibody (BD Pharmingen). For isotype controls, purified $IgG_1κ$ was used. All FACS analyses for *in vivo* fluorescence as well as surface and intracellular antigens were performed with an Epics XL (Beckman-Coulter) using the evaluation program EXPO32ADC.

Confocal microscopic analysis. Immunostaining was performed according to standard protocols, as described previously[28]. EB outgrowths seeded on 12 mm gelatin-coated glass coverslips were rinsed with PBS fixed for 20 min at room temperature with 3.7% formaldehyde and neutralized with 50 mM glycine. The cells were permeabilized using 0.4% Triton X-100 in PBS and incubated with the primary antibody in a humidified chamber at 37 °C for 2 h. After washing with 0.4% Triton X-100 and PBS, secondary Cy3-conjugated antibody was added and the specimens were incubated for 2 h at 37 °C. Finally, the cells were washed and mounted with Mowiol (Calbiochem).

Electrophysiological analysis. Isolation and electrophysiological analysis of spontaneously beating cardiac cells from EB was performed based on methods described previously[28]. Preparation and analysis of mouse embryonic cardiomyocytes, developmental day 10, was performed as described previously[29]. Please refer to Supplementary Methods for a detailed description.

Electron microscopy. For electron microscopy, the cells were cultivated on gelatine-coated tissue slides until day 12 of differentiation, fixed in 6.25% glutaraldehyde in Soerensen-Phosphate buffer, stained in 2% osmium (in aqua dest. for 1 h), dehydrated in acetone and embedded in epon. By heat-

ing, the polymerized epon plate was snipped off from the tissue slide for cutting ultra thin sections, which were counterstained with uranyl acetate and lead citrate.

ChIP assays. For ChIP assays, transfected cells were fixed in 1% formaldehyde and quenched in 0.125 M glycine. For subsequent cloning of precipitated fragments, further processing was performed as described previously[15]. For PCR (after ChIP assays) primers corresponded to the mouse *Dkk-1* promoter regions (-2.2 kb region: upper primer: 5′-GAATATGGGGAGAGAAGTGG-3′; lower primer: 5′-CAGCATACTACTAGCAATGTC-3′; -3.8 kb Region: upper primer: 5′-GCTTGTCTATCACGATGAGC-3′; lower primer: 5′-GCAAAGATTTCCCGTTCCTG-3′). All ChIP samples were tested for false-positive PCR amplification using primers amplifying 125 bp from the *H4* gene (for genomic DNA contamination).

Electrophoretic mobility shift assays (EMSAs). EMSAs were performed according to the manufacturer's protocol (Pierce) using nuclear extracts from transfected cells. Oligonucleotide sequences used for labelled EMSA probes and 100× specific competition were: mDkk-1 (-3.8 kb): GTCGAGGAGAAAGCATATGCTTTT TATTAAAC; mDkk-1 (-2.2 kb): GAGAGAAGTGGCACATATGTGTATTTC TAGG. For non-specific 100× competition oligonucleotides were: mDkk-1us (-3.8 kb): GTCGAGGAGAAAGaaaATGCTTTTTATTAAAC; mDkk-1us (-2.2 kb): GAGAGAAGTGGCAaaaATGTGTATTTCTAGG. Lower-case letters represent mutations in the bHLH motifs.

Note: Supplementary Information is available on the Nature Cell Biology website.

ACKNOWLEDGEMENTS

We are very grateful for expert technical assistance from Christiane Gross who is funded by the Deutsche Forschungsgemeinschaft (DFG; FR 705/11-3) and the Fritz-Bender-Stiftung. We are also very grateful to Frank Ebel (Max-von-Pettenkofer-Institut, Munich) for helping with the laser scanning microscopy experiments. R.D. is funded exclusively by the DFG (FR 705/11-3). C.B. and F.S. is funded by the FöFoLe program of the LMU Munich. H.L. is supported by an Emmy-Noether Fellowship of the DFG. Additional funding was granted by the Helmut Legalotz-Stiftung for FACS and consumables. We thank Christof Niehrs for the mouse Dkk-1 *in situ* probe and Yumiko Saga for providing us with the MesP1/2 dKO. embryos.

AUTHOR CONTRIBUTIONS

R. D. designed the experiments together with W.-M. F. and performed promoter studies; J. M.-H. perfromed the electron mcroscoy analyses; R. R., R. D. and E. M. performed the *Xenopus* experiments; R. D. and C. B. performed the molecular cloning and ES cell experiments, and RT-PCR; C. B., F. S. and S. B. performed the FACS and immunostaining; J. S. performed the electrophysiological studies; H. L., M. V. and S. K. performed the wild-type and knockout *in situ* hybridization studies.

Published online at http://www.nature.com/naturecellbiology/
Reprints and permissions information is available online at http://npg.nature.com/reprintsandpermissions/

1. Saga, Y. *et al.* MesP1 is expressed in the heart precursor cells and required for the formation of a single heart tube. *Development* **126,** 3437–3447 (1999).
2. Saga, Y., Kitajima, S. & Miyagawa-Tomita, S. MesP1 expression is the earliest sign of cardiovascular development. *Trends Cardiovasc. Med.* **10,** 345–352 (2000).
3. Kitajima, S., Miyagawa-Tomita, S., Inoue, T., Kanno, J. & Saga, Y. MesP1-nonexpressing cells contribute to the ventricular cardiac conduction system. *Dev. Dyn.* **235,** 395–402. (2006).
4. Maltsev, V. A., Wobus, A. M., Rohwedel, J., Bader, M. & Hescheler, J. Cardiomyocytes differentiated in vitro from embryonic stem cells developmentally express cardiac-specific genes and ionic currents. *Circ. Res.* **75,** 233–244. (1994).
5. Nir, S. G., David, R., Zaruba, M., Franz, W. M. & Itskovitz-Eldor, J. Human embryonic stem cells for cardiovascular repair. *Cardiovasc. Res.* **58,** 313–323 (2003).
6. David, R., Groebner, M. & Franz, W. M. Magnetic cell sorting purification of differentiated embryonic stem cells stably expressing truncated human CD4 as surface marker. *Stem Cells* **23,** 477–482 (2005).
7. Saga, Y. *et al.* MesP1: a novel basic helix-loop-helix protein expressed in the nascent mesodermal cells during mouse gastrulation. *Development* **122,** 2769–2678 (1996).
8. Satou, Y., Imai, K. S. & Satoh, N. The ascidian *MesP* gene specifies heart precursor cells. *Development.* **131,** 2533–2541. (2004).
9. Davidson, B., Shi, W. & Levine, M. Uncoupling heart cell specification and migration in the simple chordate *Ciona intestinalis. Development* **132,** 4811–4818 (2005).
10. Wobus, A. M. *et al.* Retinoic acid accelerates embryonic stem cell-derived cardiac differentiation and enhances development of ventricular cardiomyocytes. *J. Mol. Cell. Cardiol.* **29,** 1525–1539 (1997).
11. Kanno, S. *et al.* Nitric oxide facilitates cardiomyogenesis in mouse embryonic stem cells. *Proc. Natl Acad. Sci. USA* **101,** 12277–12281 (2004).
12. Schroeder, T. *et al.* Recombination signal sequence-binding protein Jκ alters mesodermal cell fate decisions by suppressing cardiomyogenesis. *Proc. Natl Acad. Sci. USA* **100,** 4018–4023 (2003).
13. Tillet, E. *et al.* N-cadherin deficiency impairs pericyte recruitment, and not endothelial differentiation or sprouting, in embryonic stem cell-derived angiogenesis. *Exp. Cell Res.* **310,** 392–400 (2005).
14. Kinder, S. J. *et al.* The organizer of the mouse gastrula is composed of a dynamic population of progenitor cells for the axial mesoderm. *Development* **128,** 3623–3634 (2001).
15. Weinmann, A. S. & Farnham, P. J. Identification of unknown target genes of human transcription factors using chromatin immunoprecipitation. *Methods* **26,** 37–47 (2002).
16. Izumi, N., Era, T., Akimaru, H., Yasunaga, M. & Nishikawa, S. Dissecting the molecular hierarchy for mesendoderm differentiation through a combination of embryonic stem cell culture and RNA interference. *Stem Cells* **25,** 1664–1674 (2007).
17. Sakurai, H. *et al. In vitro* modeling of paraxial and lateral mesoderm differentiation reveals early reversibility. *Stem Cells* **24,** 575–586 (2006).
18. Liu, Y. *et al.* Sox17 is essential for the specification of cardiac mesoderm in embryonic stem cells. *Proc. Natl Acad. Sci. US.* **104,** 3859–3864 (2007).
19. Kitajima, S., Takagi, A., Inoue, T. & Saga, Y. MesP1 and MesP2 are essential for the development of cardiac mesoderm. *Development* **127,** 3215–3226 (2000).
20. Foley, A. C. & Mercola, M. Heart induction by Wnt antagonists depends on the homeodomain transcription factor Hex. *Genes Dev.* **19,** 387–396 (2005).
21. Klaus, A., Saga, Y., Taketo, M. M., Tzahor, E. & Birchmeier, W. Distinct roles of Wnt/β-catenin and Bmp signalling during early cardiogenesis. *Proc. Natl Acad. Sci. USA* **104,** 18531–18536 (2007).
22. Schneider, V. A. & Mercola, M. Wnt antagonism initiates cardiogenesis in *Xenopus laevis. Genes Dev.* **15,** 304–315 (2001).
23. Eisenberg, L. M. & Eisenberg, C. A. Wnt signal transduction and the formation of the myocardium. *Dev. Biol.* **293,** 305–315 (2006).
24. Jaspard, B., Couffinhal, T., Dufourcq, P., Moreau, C. & Duplaa, C. Expression pattern of mouse sFRP-1 and mWnt-8 gene during heart morphogenesis. *Mech. Dev.* **90,** 263–267 (2000).
25. Reiter, J. F. *et al.* Gata5 is required for the development of the heart and endoderm in zebrafish. *Genes Dev.* **13,** 2983–2995 (1999).
26. David, R., Joos, T. O. & Dreyer, C. Anteroposterior patterning and organogenesis of *Xenopus laevis* require a correct dose of germ cell nuclear factor (xGCNF). *Mech. Dev.* **79,** 137–152. (1998).
27. Weintraub, H. *et al.* The *myoD* gene family: nodal point during specification of the muscle cell lineage. *Science* **251,** 761–766 (1991).
28. Muller, M. *et al.* Selection of ventricular-like cardiomyocytes from ES cells *in vitro. Faseb J.* **14,** 2540–2548 (2000).
29. Stieber, J. *et al.* The hyperpolarization-activated channel HCN4 is required for the generation of pacemaker action potentials in the embryonic heart. *Proc. Natl Acad. Sci. USA* **100,** 15235–15240 (2003).

J Membrane Biol (2007) 217:105–113
DOI 10.1007/s00232-007-9042-z

Membrane Channel Connexin 32 Maintains $Lin^-/c\text{-}kit^+$ Hematopoietic Progenitor Cell Compartment: Analysis of the Cell Cycle

Yoko Hirabayashi · Byung-Il Yoon · Isao Tsuboi · Yan Huo · Yukio Kodama · Jun Kanno · Thomas Ott · James E. Trosko · Tohru Inoue

Received: 30 April 2007 / Accepted: 14 May 2007 / Published online: 15 July 2007

Abstract Membrane channel connexin (Cx) forms gap junctions that are implicated in the homeostatic regulation of multicellular systems; thus, hematopoietic cells were assumed not to express Cxs. However, hematopoietic progenitors organize a multicellular system during the primitive stage; thus, the aim of the present study was to determine whether Cx32, a member of the Cx family, may function during the primitive steady-state hematopoiesis in the bone marrow (BM). First, the numbers of mononuclear cells in the peripheral blood and various hematopoietic progenitor compartments in the BM decreased in Cx32-knockout (KO) mice. Second, on the contrary, the number of primitive hematopoietic progenitor cells, specifically the $Lin^-/c\text{-}kit^+/Scal^+$ fraction, the KSL progenitor cell compartment, also increased in Cx32-KO mice. Third, expression of Cx32 was detected in $Lin^-/c\text{-}kit^+$ hematopoietic progenitor cells of wild-type mice (0.27% in the BM), whereas it was not detected in unfractionated wild-type BM cells. Furthermore, cell-cycle analysis of the fractionated KSL compartment from Cx32-KO BM showed a higher ratio in the G_2/M fraction. Taken together, all these results imply that Cx32 is expressed solely in the primitive stem cell compartment, which maintains the stemness of the cells, i.e., being quiescent and noncycling; and once Cx32 is knocked out, these progenitor cells are expected to enter the cell cycle, followed by proliferation and differentiation for maintaining the number of peripheral blood cells.

Keywords Connexin 32 · Hematopoiesis · Hematopoietic stem cell · Cx32-knockout mouse

Y. Hirabayashi (✉) · B.-I. Yoon · I. Tsuboi · Y. Huo · Y. Kodama · J. Kanno
Division of Cellular and Molecular Toxicology, Center for Biological Safety and Research, National Institute of Health Sciences, 1-18-1 Kamiyohga, SetagayakuTokyo 158-8501, Japan
e-mail: yokohira@nihs.go.jp

B.-I. Yoon
Laboratory of Histology and Molecular Pathogenesis, School of Veterinary Medicine, Kangwon National University, Chuncheon 200-701, Republic of Korea

T. Ott
Service Einrichtung Transgene Tiere, Hertie-Institut für Klinische Hirnforschung, Tübingen 72076, Germany

J. E. Trosko
Department of Pediatrics and Human Development, Michigan State University, College of Human Medicine, East Lansing, MI 48824, USA

T. Inoue
Center for Biological Safety and Research, National Institute of Health Sciences, Tokyo 158-8501, Japan

Introduction

Connexin (Cx) functions in the organization of cell-cell communication via gap junctions in multicellular organisms. Gap junctions have been implicated in the homeostatic regulation of various cellular functions, including growth control and differentiation (Loewenstein, 1979), apoptosis (Wilson, Close & Trosko, 2000) and the synchronization of electrotonic and metabolic functions (Bruzzone, White & Paul, 1996).

The role of Cxs in hematopoietic organs is poorly understood, except that the expression of Cx43 between hematopoietic progenitor cells and bone marrow (BM) stromal cells sustains hematopoiesis (Rosendaal, Gregan & Green, 1991; Ploemacher et al., 2000; Cancelas et al.,

2000; Montecino-Rodriguez, Leathers & Dorshkind, 2000). As Cxs are essential molecules for multicellular organisms, Cxs that organize cell-cell communication within the hematopoietic progenitor cell compartment are surmised to be present in BM tissue. If Cxs are present among hematopoietic progenitor cells, what would be their functions?

Krenacs & Rosendaal (1998) previously reported that Cx32 is not expressed in the BM. Therefore, if Cx32 is expressed in the blood cells, such Cx32-expressing cells would likely be, e.g., solely hematopoietic stem/progenitor cells. Such a specific study was supposed to be supported by the use of knockout (KO) mice for specific Cx molecules. Consequently, we found a functional impairment of the BM in Cx32-KO mice in our benzene exposure experiment (Yoon et al., 2004).

Cx32-KO mice were first established in 1996 by Willecke (Nelles et al., 1996). Using these Cx32-KO mice, an analysis of the possible functions of Cx32 in hematopoietic stem/progenitor cells was conducted using a reverse biological approach. Cx32-KO mice showed decreased numbers of peripheral mononuclear cells, various progenitor cell compartments and an increased primitive stem cell fraction, such as the lineage marker-negative (Lin^-)/c-kit-positive (c-kit^+)/stem cell antigen-1-positive ($Sca1^+$) (=KSL) fraction. On the contrary, in wild-type mice, expression of Cx32 was detected by immunocytochemistry and reverse transcriptase-polymerase chain reaction (RT-PCR), although it was not detected in unfractionated wild-type BM cells. Subsequent cell-cycle analyses, one for colony-forming progenitors using the method for evaluation of cycling progenitor cells with incorporation of bromodeoxyuridine (BrdUrd) followed by exposure to ultraviolet A (UVA) (see, BUUV Assay in Materials and Methods) and the other using a cell sorter with Hoechst 33342 for the KSL fraction, showed a significant increase in the ratio of the cell-cycle fraction in both compartments in the BM of Cx32-KO mice. The functions of Cx32, which is expressed in primitive hematopoietic stem/progenitor cells, are likely restoration of stem/progenitor cell quiescence and maintenance of primitive stem cells to prevent exhaustion.

Materials and Methods

Experimental Animals

Cx32-KO mice ($Cx32^{-/-}$ or $Cx32^{-/Y}$) were genetically modified from the F_1 embryonic cell line 129/J and the C57BL/6 strain developed by Willecke (Nelles et al., 1996). Heterozygous mice ($Cx32^{-/+}$) backcrossed with the C57BL/6 strain and maintained at the animal facility of the National Institute of Health Sciences (NIHS), Tokyo, Japan, were used. The pups were genotyped by PCR for screening of DNA from their tails.

Eight-week-old C57BL/6 male mice from Japan SLC (Hamamatsu, Japan) were used for the colonization assay. All experimental protocols involving laboratory mice in this study were reviewed by a peer review panel, the Interdisciplinary Monitoring Committee for the Right Use and Welfare of Experimental Animals, established at the NIHS, and approved by the Committee for Animal Care and Use at the NIHS with the experimental code 224-37009639415-2002.

Blood and BM Separation

The numbers of peripheral white blood cells, platelets and red blood cells were measured using a Coulter counter (Sysmex K-4500; Sysmex, Kobe, Japan). BM cells were harvested from the femur of each mouse (Yoon et al., 2001) after the animals were killed by cervical dislocation under deep anesthesia with ethyl ether. A 26-gauge needle was inserted into the femoral bone cavity through the proximal and distal ends of the bone shafts, and BM cells were flushed out under pressure by injecting 2 ml of α-minimum essential medium (α-MEM) with ribonucleosides and deoxyribonucleosides (Invitrogen, Carlsbad, CA).

Antibodies and Immunomagnetic Bead Separation

For the depletion of differentiated (lineage marker-positive) cells from BM cells, immunomagnetic bead separation (BD IMag Mouse Hematopoietic Progenitor Cell Enrichment™ set; BD Biosciences, San Jose, CA) or immunobead density gradient separation (SpinSep™; StemCell Technologies, Vancouver, Canada) was performed. As for lineage (Lin) markers, a biotinylated antibody cocktail (BD Biosciences) containing anti-mouse CD3e (145-2C11), CD11b (M1/70), CD45R/B220 (RA3-6B2), Ly-6G and Ly-6C/Gr-1 (RB6-8C5) and TER-119/erythroid cell (TER-119) antibodies and a monoclonal antibody cocktail (SpinSep) containing anti-CD5/Ly-1, CD45R, CD11b/Mac-1, Ly-6G/Gr-1, TER119 and 7/4/neutrophil antibodies were used. As a secondary antibody for the former biotinylated antibody cocktail, streptavidin (StAv)-coated beads (BD Biosciences) for depletion and StAv-peridinin chlorophyll-a protein (PerCP, BD Biosciences) for visualization were used. For the latter cocktail (SpinSep), an optimized combination antibody cocktail against it that had been coated on dense microparticles, i.e., SpinSep Mouse Dense Particles (StemCell Technologies), was used for immunoprecipitation.

For enrichment of the c-kit^+ fraction by immunomagnetic bead separation, CD117/c-kit-conjugated phycoerythrin (PE, StemCell Technologies) was used as a progenitor

marker and, as a secondary antibody, an anti-PE tetrameric antibody complex (StemCell Technologies) was used.

For detection of Cx32-positive cells by flow cytometry, a mouse anti-Cx32 monoclonal antibody from two sources (Chemicon International, Temecula, CA; Santa Cruz Technology, Santa Cruz, CA) as a primary antibody and an anti-mouse immunoglobulin (Ig) conjugated with fluorescein isothiocyanate (FITC) as a secondary antibody (BD Biosciences) were used.

For cell-cycle analysis by flow cytometry, as lineage markers, the same antibody cocktails from BD Biosciences were used. In addition, CD117/c-kit conjugated with allophycocyanin (APC), stem cell antigen (Sca1) antibody conjugated with PE and an AT-rich DNA-binding dye, Hoechst 33342 (Sigma, St. Louis, MO), were used.

Immunohistochemical Analysis

The same anti-Cx32 antibody (Chemicon International) was used as the primary antibody. As for the secondary antibody, a biotinylated horse anti-mouse Ig G (Vector Laboratories, Burlingame, CA) was used, and streptavidin labeled with peroxidase and 3,3′-diaminobenzidine was used to detect immunoreactivity (Vector Laboratories).

Enrichment of BM Cells in $Lin^-/c\text{-}kit^+$ Fraction

The $Lin^-/c\text{-}kit^+$ fraction is rich in hematopoietic stem cells (HSCs). To obtain a large number of $Lin^-/c\text{-}kit^+$ progenitor cell-enriched fraction in BM cells, a combination of immunobead density gradient and immunomagnetic bead separation techniques was carried out. First, for the depletion of lineage-positive BM cells, harvested BM cells were processed through an immunobead density gradient using a density-matched medium and dense microparticles coated with a cocktail of an optimized combination of antibodies called SpinSep (StemCell Technologies). Second, for the selection of the $c\text{-}kit^+$ fraction, immunomagnetic bead separation using magnetic nanoparticles with a magnetic holder was carried out according to the manufacturer's instruction (StemCell Technologies). For each procedure, the antibodies used are described under Antibodies and Immunomagnetic Bead Separation, above.

Flow-Cytometric Analysis using Anti-Cx32 Antibody

BM cells with or without fractionation for $Lin^-/c\text{-}kit^+$ HSC enrichment were stained with the biotinylated antibody cocktail of StAv-PerCP, c-kit-PE, the anti-Cx32 antibody and anti-mouse IgG conjugated with FITC. Flow-cytometric analysis was carried out using FACSVantage and FACSAria (both from BD Biosciences).

Flow-Cytometric Analysis for Cell Cycle of KSL Fraction

Lineage-depleted BM cells were stained with the biotinylated antibody cocktail with StAv-PerCP, c-kit-APC, Sca1-PE and Hoechst 33342. Flow-cytometric analysis was carried out using FACSAria.

BUUV Assay

Hematopoietic progenitor cell-specific kinetic studies were evaluated by continuous labeling by an osmotic minipump (Alza, Palo Alto, CA) of BrdUrd for cycling cells, followed by UVA exposure and hematopoietic colonization assay (BUUV assay, details in Hirabayashi et al., 1998, 2002).

Irradiation

In the assay of hematopoietic progenitor cells, recipient mice were exposed to a lethal radiation dose of 915 cGy, at a dose rate of 124 cGy per minute, using a ^{137}Cs-gamma irradiator (Gammacell 40 Exactor; MDS Nordin, Ottawa, Canada) with a 0.5-mm aluminum-copper filter.

Assay for Colony-Forming Units in Spleen

The Till & McCulloch (1961) method was used to determine the number of hematopoietic spleen colonies, i.e., colony-forming units in spleen (CFU-S), formed by hematopoietic progenitor cells. Aliquots of a BM cell suspension were used for evaluating the numbers of CFU-S. Spleens were harvested 9 or 13 days after BM transplantation for determining the number of CFU-S-9 or CFU-S-13 and then fixed in Bouin's solution. Macroscopic spleen colonies were counted under an inverted microscope at ×5.6. It was previously shown, using the C57BL/6 strain, that all colonies visible on days 9 and 13 originate from transplanted BM cells under the condition that the recipient mice are exposed to a lethal radiation dose of 915 cGy (Hirabayashi et al., 2002).

Assay for Granulocyte-Macrophage Colony-Forming Units

Granulocyte-macrophage colony-forming units (CFU-GM) were assayed in semisolid methylcellulose culture (Yoon et al., 2001; Hirabayashi et al., 2002). Briefly, 8×10^4 BM cells suspended in 100 μl of α-MEM were added to 3.9 ml of culture medium containing 1% methylcellulose (Nakarai-Tesque, Kyoto, Japan), 30% fetal calf serum (HyClone Laboratories, Logan, UT), 1% bovine serum albumin (Sigma), 10^{-4} M mercaptoethanol (Sigma) and 10 ng/ml murine granulocyte-macrophage

colony-stimulating factor (GM-CSF; R&D Systems, Minneapolis, MN). One-milliliter aliquots containing 2×10^4 cells were placed in 35-mm tissue culture wells (Nalgen Nunc International, Rochester, NY) in triplicate and incubated for 6 days in a fully humidified incubator at 37°C with 5% CO_2 in air. Colonies were counted using an inverted microscope at ×40 (Olympus Optical, Tokyo, Japan).

PCR Analysis for Genotyping

To detect Cx32 wild-type and Cx32-KO alleles, PCR analysis was performed using genomic DNA from the tail of each mouse, and synthetic oligonucleotides were used as primers (Nelles et al., 1996). To detect the wild-type allele, a 5′ primer (ccataagtcaggtgtaaaggagc) and a 3′ primer (agataagctgcagggaccatagg) were used; to detect the Cx32-KO allele, a common 5′ primer and a *neo*-primer (atcatgcgaaacgatcctcatcc) were used.

Reverse Transcription and PCR Analysis of Cx32 Expression

Expression of the gene encoding Cx32 was analyzed by reverse transcription followed by PCR. The total RNA from BM cells and other tissues was isolated using a Qiagen RNAeasy kit (Qiagen, Valencia, CA).

Statistical Analysis

The data obtained were stored in a computer and processed for statistical analysis using Student's *t*-test to evaluate the significance of differences in blood cell count, BM cellularity and the numbers of progenitor cells, CFU-GM, CFU-S-9 and CFU-S-13 between the wild-type group and the KO group. Differences with $p < 0.05$ were considered significant.

Results

Expression of Cx32 in Bone Marrow

Table 1 shows various blood cell parameters for the wild-type and Cx32-KO mice, with body weight and spleen weight as references. Although the total numbers of BM cells and red blood cells did not significantly differ between the wild-type mice and the Cx32-KO mice, the numbers of white blood cells and platelets from the peripheral blood, CFU-S-13 (primitive hematopoietic progenitor cells), CFU-S-9 (differentiated progenitor cells) and CFU-GM (progenitor cells cultured *in vitro*) were all significantly lower in the Cx32-KO mice than in the wild-type mice. These results suggest that the Cx32-KO mice have a potential disadvantage in hematopoiesis. However, when we studied the expression of Cx32 in BM cells by RT-PCR, as shown in Figure 1, neither the expression of Cx32 in the spleen (*not shown*) nor that in the BM was detected except in the positive known control, the hepatic tissue. Thus, the negative expression of Cx32 in BM cells is in good agreement with a previous observation (Krenacs & Rosendaal, 1998).

Table 1 Parameters associated with steady-state hematopoiesis

Parameter	Wild-type	Cx32-KO
Body weight (g)	22.6 ± 1.97	22.5 ± 1.77
Spleen weight (mg)	77.8 ± 17.7	88.3 ± 9.6
BM cellularity ($\times 10^7$/femur)	2.28 ± 0.23	2.15 ± 0.08
Peripheral blood cells		
Red ($\times 10^7$/ml)	960 ± 30.8	930 ± 50.4
White ($\times 10^4$/ml)*	7,300 ± 283	5,633 ± 569
Platelets ($\times 10^7$/ml)*	67.6 ± 0.14	48.7 ± 0.93
Hematopoietic progenitor cells		
CFU-GM ($\times 10^2$/femur)*	387 ± 33.5	251 ± 27.4
CFU-S-9 ($\times 10^2$/femur)*	45.8 ± 4.78	32.7 ± 5.23
CFU-S-13 ($\times 10^2$/femur)*	27.7 ± 3.35	21.1 ± 2.85

Each value is expressed as average ($n = 6$ for each genotype) ± standard deviation except for the value of the hematopoietic progenitor cells. The numbers of hematopoietic progenitor cells in steady-state CFU-GM, day-9 spleen colonies (CFU-S-9) and day-13 spleen colonies (CFU-S-13) are expressed as average (three donor mice were used for each genotype, and six mice were used for each recipient group) ± standard deviation

* The difference calculated by *t*-test between wild-type and Cx32-KO is significant ($p < 0.05$)

We next studied Cx32 expression in colonies developed in the spleen in lethally irradiated wild-type recipient mice after injection of BM cells from wild-type mice or from Cx32-KO mice. Hematopoietic spleen colonies consist of a large number of immature cells rather than cells from the peripheral blood or unfractionated BM cells (Hirabayashi et al., 2002). Expression of Cx32 detected by RT-PCR analysis was only observed in the hematopoietic spleen colonies derived from wild-type BM cells (Fig. 1, lanes A1, A2). Expression of Cx32 was not detected in colonies derived from Cx32-KO BM cells, which are negative controls (Fig. 1, lanes B1, B2). Expression of Cx32 was also detected in spleen colonies from Cx32-KO recipient mice that had been repopulated with wild-type BM cells (Fig. 1, lanes C1, C2).

Immunohistochemical staining with the anti-Cx32 antibody was carried out to examine the hematopoietic spleen colonies originating from BM cells from wild-type mice and from Cx32-KO mice. A colony originating from a wild-type BM cell showed mild and mottled staining in the outer boundary of the spleen colonies, whereas a colony originating from Cx32-KO BM cells showed no staining

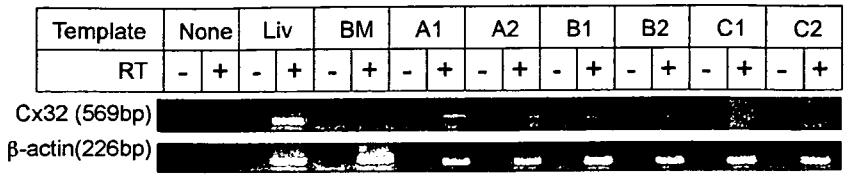

Fig. 1 Expression of Cx32 in BM and hematopoietic spleen colonies. Total RNAs were extracted for RT-PCR from the liver (*Liv*) and BM of wild-type mice and CFU-S-9. Note that Cx32 expression was not detected in the BM but was detected in the liver, which is a positive control (see Materials and Methods). To obtain CFU-S, lethally irradiated wild-type mice were injected with BM cells from wild-type or Cx32-KO donor mice. After 9 days, total RNAs extracted from individual hematopoietic spleen colonies derived from wild-type BM cells or those from Cx32-KO BM cells were reverse-transcribed, followed by PCR and then loaded (lanes *A1, A2, C1* and *C2*). Also, total RNAs extracted from the colonies derived from wild-type BM cells obtained from lethally irradiated Cx32-KO recipient mice followed by repopulation with wild-type BM cells were similarly loaded (lanes *B1* and *B2*). RT(+) and RT(-): with or without avian reverse transcriptase, 2.5 U/20 μl, respectively (see Materials and Methods)

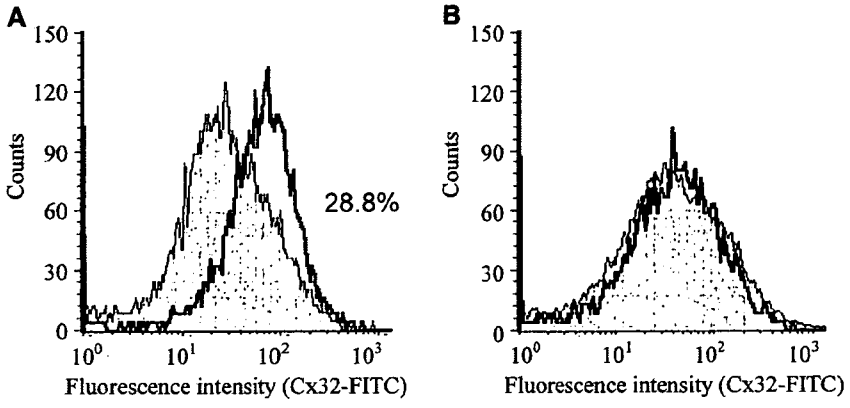

Fig. 2 Flow-cytometric analyses of $Lin^-/c\text{-}kit^+$ Cx32-positive cells from wild-type mice. Flow cytometry after BM cell separation was carried out by a combination of immunobead density gradient separation and immunomagnetic bead separation. Histogram of FITC-labeled anti-Cx32 antibody. $Lin^-/c\text{-}kit^+$ fraction (**a**) and $Lin^+/c\text{-}kit^-$ fraction (**b**) for wild-type BM cells (*open profile with bold line*) and same fractions for Cx32-KO BM cells (*shaded profile*), negative control. The Cx32-positive fraction shown in **a** calculated for the $Lin^-/c\text{-}kit^+$ fraction in wild-type BM cells is 28.8%

(*data not shown*). The findings described above suggest expression of Cx32 in the hematopoietic progenitor cells or stem cells alone; thus, further precise experiments were conducted.

Expression of Cx32 in $Lin^-/c\text{-}kit^+$ Hematopoietic Progenitor Cell Compartment

We determined whether Cx32-positive cells are consistently found in the HSC compartment. First, the $Lin^-/c\text{-}kit^+$ HSC-enriched fraction was obtained by the combination of immunobead density gradient separation for depleting lineage-positive cells and immunomagnetic bead separation for selecting $c\text{-}kit^+$ cells, followed by flow-cytometric analysis using the anti-Cx32 antibody. The separated $Lin^-/c\text{-}kit^+$ HSC fraction was 0.25% of the original unfractionated wild-type BM cells. The proportion of the $Lin^-/c\text{-}kit^+$ compartment (HSC compartment) is 90.2% of the $Lin^-/c\text{-}kit^+$ HSC-enriched preseparated fraction. Furthermore, the number of $Lin^-/c\text{-}kit^+$ compartments is 106.9-fold higher than the fraction of the original unfractionated BM cells. To determine which fraction Cx32-positive cells belong to, BM cells from wild-type mice and Cx32-KO mice with or without $Lin^-/c\text{-}kit^+$ HSC enrichment were stained with biotinylated antibody cocktail labeled with StAv-PerCP, c-kit-PE and Cx32-FITC. In wild-type BM cells, 28.8% of the $Lin^-/c\text{-}kit^+$ fraction was found to be Cx32-positive compared with the same fraction of BM cells obtained from Cx32-KO mice, which was used as the negative control (Fig. 2a). Together with the frequency data for the $Lin^-/c\text{-}kit^+$ HSC-enriched fraction, the fraction of Cx32-positive cells was calculated to be nearly 0.27% of the original unfractionated whole BM cells.

Whether the mature cell fraction, i.e., the $Lin^+/c\text{-}kit^-$ fraction, contains Cx32-positive cells, the fraction of the wild-type BM cells is compared with that of the control profile from the Cx32-KO mice. Because both fractions are nearly identical (Fig. 2b), few cells may be positive for Cx32 in the $Lin^+/c\text{-}kit^-$ fraction. The fraction of Cx32-positive cells is 0.0093% of the original unfractionated whole BM cells (*data not shown*).

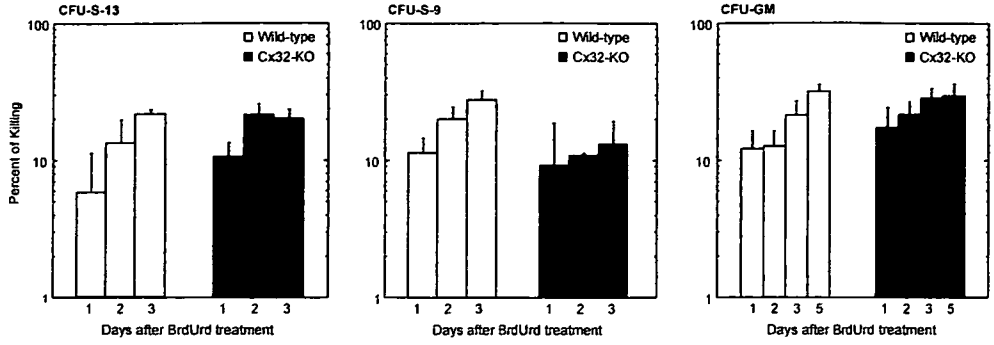

Fig. 3 The BrdUrd-labeled cells with an osmotic minipump purged by UVA light (BUUV) assay for evaluating the cycling fractions of the hematopoietic colonizing progenitor cells. Percent decreases in number of colonies compared with nonexposed control are shown along the ordinate axis (log.) vs. days for continuous labeling of BrdUrd with osmotic minipumps shown along the horizontal axis. CFU-S-13 (primitive hematopoietic progenitor cells), CFU-S-9 (differentiated progenitor cells) and CFU-GM (progenitor cells assayed by *in vitro* colonization) are shown. Each column represents 10 mice assayed for CFU-S-13 and six mice assayed for CFU-S-9

Function of Cx32 in Cell-Cycle Regulation in Hematopoietic Progenitor/Stem Cells

A significant decrease in the number of hematopoietic progenitor cells was observed in the Cx32-KO mice but without any significant difference in the decrease in BM cell number (Table 1), suggesting cell-cycle perturbation in the hematopoietic progenitor cells or stem cell compartment. Whether cell cycles are accelerated or decelerated in either the hematopoietic progenitor cell fractions or the hematopoietic stem cell compartment or both is not known. To characterize hematopoietic progenitor-specific cell cycle, the BUUV assay was conducted. To observe possible changes in the cell cycle in the hematopoietic stem cell compartment, the KSL fraction was assayed with Hoechst 33342 and possible changes in the ratio of G_0/G_1 were evaluated.

BUUV assay Hematopoietic stem cell-specific kinetics evaluation by continuous infusion of BrdUrd for cycling cells including hematopoietic progenitor cells followed by UVA exposure and hematopoietic progenitor colonization assay was conducted.

Results are shown in Figure 3. For CFU-S-13 (primitive hematopoietic progenitor cells), the incorporation of BrdUrd starts from a higher percentage with rapid increase in Cx32-KO mice, suggesting suppression of the cell cycle in these primitive hematopoietic progenitor cells with Cx32-mediated cell-cycle regulation in the wild-type steady state. This suppression may be attenuated in CFU-S-9, a differentiated progenitor cell compartment. For CFU-GM, the progenitor cells assayed by *in vitro* colonization also showed an accelerated cell cycle in Cx32-KO mice. The population doubling time calculated for each progenitor cell compartment is shown in Table 2.

Flow-cytometric analysis of KSL fraction Following the incorporation of the bioactive AT-rich DNA-binding dye Hoechst 33342, the lineage-depleted BM cells were analyzed by flow cytometry. The sizes of the $Lin^-/c\text{-}kit^+/Sca1^+$ (KSL) fraction obtained were 0.052% in the Cx32-KO BM cell compartment and 0.035% in wild-type BM cells (Table 3, Fig. 4a; $p = 0.0458 < 0.05$). The lineage-depleted BM cells were analyzed for their cell-cycle patterns by flow cytometry (Fig. 4b,c), and then G_0/G_1 was calculated for the $Lin^-/c\text{-}kit^+$ and KSL fractions for both the Cx32-KO and wild-type mice. The percentage of G_0/G_1 calculated for the $Lin^-/c\text{-}kit^+$ and KSL fractions were slightly lower in Cx32-KO mice (Table 4; 83.3% vs. 87.2% for Cx32-KO vs. wild-type for the $Lin^-/c\text{-}kit^+$ fraction, 89.2% vs. 91.5% for Cx32-KO vs. wild-type for

Table 2 Doubling times of hematopoietic progenitor cells

Progenitor cell	Genotype	Slope (%killing/day)[a]	*y* intercept (%)[a]	Population doubling[b] (h)	*r*
CFU-GM	Wild-type	0.255	9.09	28.3	0.973
	Cx32-KO	0.244	13.54	29.6	0.995
CFU-S9	Wild-type	0.440	7.62	16.4	0.986
	Cx32-KO	0.179	7.82	40.3	0.999
CFU-S13	Wild-type	0.659	3.16	11.0	0.988
	Cx32-KO	0.694	5.35	10.4	0.999

[a] Regression line: $y = b\ 10^{(ax)}$, where x is the duration after BrdUrd treatment (days), y is the percentage of killing, a is cell cycle velocity (coefficient) and b is the cycling ratio/unit time (coefficient)

[b] Doubling time (h) = (log2/a) × 24

Table 3 Incidence of hematopoietic stem cell fraction/femoral BM cells

Hematopoietic stem cell fraction	Wild-type	Cx32-KO	p*
Lin^--c-kit^+ fraction (%)	0.316 ± 0.007	0.412 ± 0.022	0.0010
KSL fraction (%)	0.035 ± 0.008	0.052 ± 0.011	0.0458

Each value is expressed as average (n = 3 for each genotype) ± standard deviation

* The difference between wild-type and Cx32-KO was calculated by t-test

the KSL fraction; $p = 0.0126$ and $p = 0.0556$, respectively). The results suggest that Cx32 may have a suppressive function on such a hematopoietic stem cell compartment, KSL, under the physiological condition of Cx32.

Discussion

The role of Cx32 in steady-state hematopoiesis was analyzed in this study. This is the first observation of a Cx gene, namely *Cx32*, that is expressed in hematopoietic stem/progenitor cells. The functions of Cx32 in hematopoiesis were also investigated. In Cx32-KO mice, the numbers of various hematopoietic progenitor cells in the BM were lower than those in wild-type mice, suggesting a beneficial role of Cx32 for maintaining hematopoiesis during the steady state. Because the cell-cycle analyses of the hematopoietic stem cells, namely, the Lin^-/c-kit^+/$Sca1^+$ KSL, or the progenitor cells, Lin^-/c-kit^+ fractions, suggested a slightly but significantly higher incidence of a dormant stem cell fraction in wild-type mice, the physiological role of Cx32 is probably to maintain

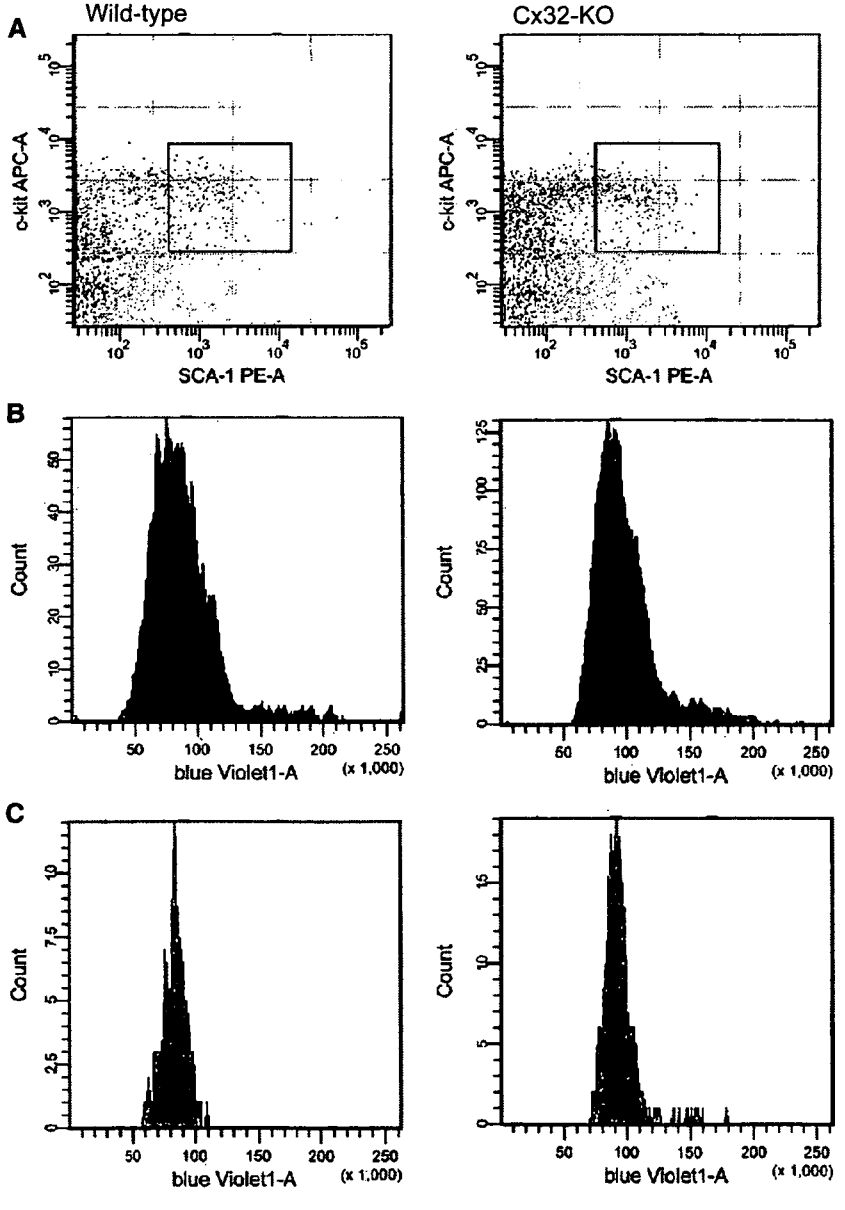

Fig. 4 **a** Two-dimensional expression shown by flow-cytometric analysis between c-kit and Sca1 expression on cells gated by lineage-negative fractions: wild-type and Cx32-KO mice. *Box* represents the c-kit^+/$Sca1^+$ fraction; thus, it is equivalent to the KSL fraction. **b**, **c** Flow-cytometric histograms showing reaction to Hoechst 33342 for Lin^-/c-kit^+ fraction (**b**) and Lin^-/c-kit^+/$Sca1^+$ (=KSL) fraction (**c**)

Table 4 G_0/G_1 ratio of hematopoietic stem cell fraction

Hematopoietic stem cell fraction	Wild-type	Cx32-KO	p^*
Lin^-/c-kit^+ fraction (%)	87.2 ± 0.76	83.3 ± 1.75	0.0126
KSL fraction (%)	91.5± 2.53	89.2 ± 1.82	0.0556

Each value is expressed as average (n = 3 for each genotype) ± standard deviation

* The difference between wild-type and Cx32-KO was calculated by t-test

the quiescence of the primitive hematopoietic stem cell compartment, thereby maintaining the stemness of the cells in the fraction.

Various Cxs are expressed in the stromal cells of the fetal liver (i.e., Cxs 43, 45, 30.3, 31 and 31.1) and the BM (i.e., Cxs 43, 45 and 31) (Cancelas et al., 2000). However, the contribution of Cxs to hematopoiesis was determined only on the basis of the effect of Cxs via stromal cell dependence; consequently, no Cxs were previously found in hematopoietic stem cells or progenitor cells (Krenacs & Rosendaal, 1998). However, in our recent study, interestingly, Cx32-KO mice exposed to benzene showed hematopoietic impairment more than wild-type mice; furthermore, the site of this impairment was not identified in either hematopoietic progenitor cells or stromal cells (Yoon et al., 2004).

Thus, we first determined whether hematopoietic progenitor cells express Cx32 molecules. As reported elsewhere (Yoon et al., 2004; Nelles et al., 1996), no Cx32 was detected in unfractionated BM cells by either RT-PCR or cell sorter analysis with an immunofluorescence antibody against Cx32 in this study (Figs. 1, 2). However, interestingly, hematopoietic spleen colonies, derived from hematopoietic progenitor cells and consisting of relatively immature hematopoietic cells, were found to express Cx32. This observation was also consistent with the immunohistochemical reaction of cells in the colonies with the anti-Cx32 antibody, in which Cx32-positive cells were only found along the border of each colony (*data not shown*). Subsequent flow-cytometric analysis using the anti-Cx32 antibody after performing the combination of immunobead density gradient separation and immunomagnetic bead separation showed that the most Cx32-positive fraction belonged to the HSC-enriched fraction, i.e., the Lin^-/c-kit^+ fraction (28.8% of the fraction) (Fig. 2a). It was calculated as only 0.27% with respect to the unseparated BM cells. Because RT-PCR or Northern blotting possibly detects >1% of expressing cells, these findings are in good agreement with a previous report on the absence of Cx32 expression in unseparated BM tissue (Cancelas et al., 2000). A hematopoietic disadvantage in progenitor cells associated with Cx32 deficiency was further evident because all progenitor cells from the BM of Cx32-KO mice showed ~20% decrease in the numbers of CFU-S-13, CFU-S-9 and CFU-GM. Thus, it can be concluded that Cx32 is required for maintaining normal hematopoiesis, specifically during the maturation of hematopoietic stem cells to progenitor cells.

BM transplantation in different combinations of the donor and recipient, which were repopulated with BM cells from either wild-type or Cx32-KO mice, showed a small number of spleen colonies in the groups repopulated with Cx32-KO BM cells (*data not shown*). Interestingly, the colonies derived from the same Cx32-KO BM cells were significantly smaller, regardless of the genotype of the recipients, i.e., wild-type or Cx32-KO mice, presumably owing to the lack of Cx32 expression in the hematopoietic progenitor cells.

Whether Cx32 is also functional in differentiated mature blood cells is, however, questionable despite the observation that the numbers of white blood cells and platelets in the peripheral blood were significantly lower in Cx32-KO than in wild-type mice (Table 1). It is interesting to calculate the probability of Cx32-positive cells on the basis of the ratio of the number of Cx32-positive BM cells to the Lin^+/c-kit^- fraction, i.e., only 0.0093% of the unfractionated original BM cells (*data not shown*). Because our repeated analysis failed to detect Cx32 expression in mature blood cells, the decreased numbers of white blood cells and platelets in the Cx32-KO mice may reflect the shortage of immature progenitor cell compartments, possibly due to the lack of Cx32 at the level of the stem and progenitor cells.

Flow-cytometric cell cycle analyses of the Lin^-/c-kit^+/$Sca1^+$, KSL fraction with Hoechst 33342 and the BUUV assay for colony-forming progenitor cells showed that the cell cycle of the hemopoietic stem cell fractions, i.e., the Lin^-/c-kit^+/$Sca1^+$, KSL or Lin^-/c-kit^+ fraction, seems to be maintained in the quiescence state, thereby maintaining the stemness of the cells, although consequent molecular regulations of these fractions are not yet known.

Acknowledgment The authors thank Dr. K. Sai, Ms. E. Tachihara, Ms. N. Moriyama, Ms. Y. Usami and Ms. M. Uchiyama for excellent technical assistance as well as Ms. N. Kikuchi, Ms. M. Yoshizawa and Ms. M. Hojo for secretarial assistance. Use of FACSAria (BD Biosciences) for flow-cytometric analysis was facilitated by Dr. H. Akiyama and Dr. T. Maitani, Division of Food Sciences, NIHS. This study was supported in part by a Grant-in-Aid for Scientific Research (B 11694334, C 16590329 and C 18510066), the Japan Society for the Promotion of Science Invitation Fellowship for Research in Japan (S01275), the Health Sciences Basic Project and the Integrated Study Project in Drug Innovation Science conducted by the Japan Health Sciences Foundation (KHC1204) and the Ministry of Health, Labour and Welfare (MHLW) Research Fund (H18-Chemistry 001), National Institute of Health Sciences.

References

Bruzzone R, White TW, Paul DL (1996) Connections with connexins: the molecular basis of direct intercellular signaling. Eur J Biochem 238:1–27

Cancelas JA, Koevoet WL, de Koning AE, Mayen AE, Rombouts EJ, Ploemacher RE (2000) Connexin-43 gap junctions are involved in multiconnexin-expressing stromal support of hemopoietic progenitors and stem cells. Blood 96:498–505

Hirabayashi Y, Matsuda M, Aizawa S, Kodama Y, Kanno J, Inoue T (2002) Serial transplantation of p53-deficient hemopoietic progenitor cells to assess their infinite growth potential. Exp Biol Med (Maywood) 227:474–479

Hirabayashi Y, Matsumura T, Matsuda M, Kuramoto K, Motoyoshi K, Yoshida K, Sasaki H, Inoue T (1998) Cell kinetics of hemopoietic colony-forming units in spleen (CFU-S) in young and old mice. Mech Ageing Dev 101:221–231

Krenacs T, Rosendaal M (1998) Connexin43 gap junctions in normal, regenerating, and cultured mouse bone marrow and in human leukemias: their possible involvement in blood formation. Am J Pathol 152:993–1004

Loewenstein WR (1979) Junctional intercellular communication and the control of growth. Biochim Biophys Acta 560:1–65

Montecino-Rodriguez E, Leathers H, Dorshkind K (2000) Expression of connexin 43 (Cx43) is critical for normal hematopoiesis. Blood 96:917–924

Nelles E, Butzler C, Jung D, Temme A, Gabriel HD, Dahl U, Traub O, Stumpel F, Jungermann K, Zielasek J, Toyka KV, Dermietzel R, Willecke K (1996) Defective propagation of signals generated by sympathetic nerve stimulation in the liver of connexin32-deficient mice. Proc Natl Acad Sci USA 93:9565–9570

Ploemacher RE, Mayen AE, De Koning AE, Krenacs T, Rosendaal M (2000) Hematopoiesis: gap junction intercellular communication is likely to be involved in regulation of stroma-dependent proliferation of hemopoietic stem cells. Hematology 5:133–147

Rosendaal M, Gregan A, Green CR (1991) Direct cell-cell communication in the blood-forming system. Tissue Cell 23:457–470

Till JE, McCulloch EA (1961) A direct measurement of the radiation sensitivity of normal mouse bone marrow cells. Radiat Res 14:213–222

Wilson MR, Close TW, Trosko JE (2000) Cell population dynamics (apoptosis, mitosis, and cell-cell communication) during disruption of homeostasis. Exp Cell Res 254:257–268

Yoon BI, Hirabayashi Y, Kawasaki Y, Kodama Y, Kaneko T, Kim DY, Inoue T (2001) Mechanism of action of benzene toxicity: cell cycle suppression in hemopoietic progenitor cells (CFU-GM). Exp Hematol 29:278–285

Yoon BI, Hirabayashi Y, Kawasaki Y, Tsuboi I, Ott T, Kodama Y, Kanno J, Kim DY, Willecke K, Inoue T (2004) Exacerbation of benzene pneumotoxicity in connexin 32 knockout mice: enhanced proliferation of CYP2E1-immunoreactive alveolar epithelial cells. Toxicology 195:19–29

Protective Role of Connexin 32 in Steady-State Hematopoiesis, Regeneration State, and Leukemogenesis

YOKO HIRABAYASHI,* BYUNG-IL YOON,*[,1] ISAO TSUBOI,* YAN HUO,* YUKIO KODAMA,* JUN KANNO,* THOMAS OTT,† JAMES E. TROSKO,‡ AND TOHRU INOUE§[,2]

*Division of Cellular and Molecular Toxicology, Center for Biological Safety and Research, National Institute of Health Sciences, Tokyo 158-8501, Japan; †Service Einrichtung Transgene Tiere, Hertie-Institut für Klinische Hirnforschung, Tübingen 72076 Germany; ‡Department of Pediatrics and Human Development, Michigan State University, College of Human Medicine, East Lansing, Michigan 48824; and §Center for Biological Safety and Research, National Institute of Health Sciences, Tokyo 158-8501, Japan

The role of gap junctions formed by connexins (Cxs) has been implicated in the homeostatic regulation of multicellular systems. Primitive hematopoietic progenitor cells form a multicellular system, but a previous report states that Cx32 is not expressed in the bone marrow. Thus, a question arises as to why Cx molecules are not detected in the hematopoietic tissue other than in stromal cells. Based on our preliminary study, which suggested a potential impairment of hematopoiesis in Cx32-knockout (KO) mice, the objectives of the present study were to determine whether Cx32 functions in the bone marrow during steady-state hematopoiesis and to examine its possible protective roles during regeneration after chemical abrasions and during leukemogenesis after the administration of a secondary genotoxic chemical, methyl nitrosourea (MNU). As a result, the Cx32 molecule, functioning in the hematopoietic stem cell (HSC) compartment during steady-state hematopoiesis, was observed for the first time; the expressions of Cx32 at the mRNA level, as determined by polymerase chain reaction analysis, and at the protein level, determined using an anti-Cx32 antibody, were observed only in the $lin^{-}c\text{-}kit^{+}$ HSC fraction, using a combination of immunobead-density gradient and immunomagnetic bead separation. Hematopoiesis was impaired in the absence of Cx32, and it was delayed during regeneration after chemical abrasion with 5-fluorouracil at 150 mg/kg body wt in Cx32-KO mice. Cx32-KO mice showed increased leukemogenicity compared with wild-type mice after MNU injection; furthermore, in a competitive assay for leukemogenicity in mice that had been lethally irradiated and repopulated with a mixed population of bone marrow cells from Cx32-KO mice and wild-type mice, the resulting leukemias originated predominantly from Cx32-KO bone marrow cells. In summary, the role of Cx32 in hematopoiesis was not previously recognized, and Cx32 was expressed only in HSCs and their progenitor cells. The results indicate that Cx32 in wild-type mice protects HSCs from chemical abrasion and leukemogenic impacts. Exp Biol Med 232:700–712, 2007

Key words: connexin 32 (Cx32); hematopoietic stem cell; Cx32-knockout mouse; tumor suppressor; experimental leukemogenesis

Introduction

Connexin (Cx) functions in the organization of cell-cell communication *via* gap junctions in multicellular organisms. Gap junctions have been implicated in the homeostatic regulation of various cellular functions, including growth control and differentiation (1), apoptosis (2), and the synchronization of electrotonic and metabolic functions (3).

Radiation exposure and acute tissue injury induce the disconnection of Cxs, resulting in tissue damage (4). On the other hand, the disconnection of Cxs during acute-phase cellular injury also seems to be a protective response that results in active tissue proliferation and consequent recovery. However, transgenic mice expressing a dominant-negative mutant of Cx32 show a notably delayed recovery after partial hepatectomy compared with wild-type mice (5), which implies that the downmodulation of Cx32 is not always advantageous for tissue recovery, despite the

This study was supported by a Grant-in-Aid for Scientific Research B, 11694334, and also by the Japanese Society for the Promotion of Science (JSPS) Invitation Fellowship for Research in Japan, S01275.

[1] Current address: Department of Veterinary Medicine, College of Animal Resource, Kangwon National University, Chuncheon, 200-701, Republic of Korea.

[2] To whom correspondence should be addressed at 1-18-1 Kamiyohga, Setagayaku, Tokyo 158-8501, Japan;. E-mail: tohru@nihs.go.jp

Received July 15, 2006.
Accepted December 7, 2006.

1535-3702/07/2325-0700$15.00

finding that a lack of gap junctional restriction seems to enhance cell proliferation (6) (see also Ref. 7 for current information).

Gap junctions are downmodulated during an acute exposure to promoter chemicals, the carcinogenic relevance of which is as yet not clearly understood (8). Temme *et al.* found that not only spontaneous hepatic tumors but also diethyl-nitrosamine–induced tumors are preferentially induced in Cx32-knockout (KO) mice compared with wild-type mice (9). Why does the downmodulation of Cxs attenuate the protection from malignancy? The reason is that the downmodulation of Cxs results in individual potentially transformable initiated cells that are undergoing independent and infinite growth without interference from surrounding cells; thus, the downmodulation of Cxs in this case seems unlikely to play a protective role (6). On the other hand, the downmodulation of Cxs after exposure to a possible carcinogenic chemical, cadmium, induces cells to undergo apoptosis, which appears to be a protective role (10), though not all cells undergo apoptosis, unfortunately.

The role of Cxs in hematopoietic organs is poorly understood, except in that the expression of Cx43 between hematopoietic progenitor cells and bone marrow stromal cells sustains hematopoiesis (11–14). As Cxs are essential molecules for multicellular organisms, Cxs that organize cell-cell communication within the hematopoietic progenitor cell compartment are surmised to be present in the bone marrow tissue. Recently, we have observed a functional impairment of the bone marrow in Cx32-KO mice in our benzene exposure experiment (15). Krenacs and Rosendaal previously reported that Cx32 is not expressed in the bone marrow (16). If Cx32 is expressed, such Cx32-expressing cells are likely to be rare; for instance, solely in hematopoietic stem/progenitor cells. Hence, similarly to the case of transforming growth factor-β expression, which is observed only in an immature progenitor cell compartment of the bone marrow (17, 18), it seems to be worth studying the expression of Cx32 in the hematopoietic system, particularly in hematopoietic stem/progenitor cells. In this study, we determined whether Cx32 functions solely in primitive hematopoietic cells in a steady-state bone marrow to elucidate its potential protective role during regeneration after bone marrow abrasion and during leukemogenesis after the administration of a secondary genotoxic chemical, methylnitrosourea (MNU).

Cx32-KO mice, first established in 1997 by Nelles *et al.*, can be used for the analysis of the function of Cx32 using a reverse biologic approach (19). In using these mice, the contribution of Cx32, not only in steady-state hematopoiesis and regenerating hematopoiesis but also in the prevention/suppression of leukemogenesis, was elucidated.

Materials and Methods

Experimental Animals. Cx32-KO mice ($Cx32^{-/-}$ or $Cx32^{-/Y}$) were genetically modified from the F1 embryonic cell line, 129/J, and the C57BL/6 strain by K. Willecke (19), who kindly provided these Cx32-KO mice, which were backcrossed with the C57BL/6 strain, and maintained as heterozygous mice ($Cx32^{-/+}$) at the animal facility of the National Institute of Health Sciences (NIHS), Japan. Because the *Cx32* gene is X chromosome linked, male mice carrying the homozygous knockout genotype ($Cx32^{-/Y}$) were generated by mating heterozygous females ($Cx32^{-/+}$) with wild-type males ($Cx32^{+/Y}$). The pups were genotyped by polymerase chain reaction (PCR) screening of DNA obtained from their tails.

Eight-week-old C57BL/6 female mice from Japan SLC (Hamamatsu, Japan) were used as the recipients of bone marrow transplantation. All experimental protocols involving laboratory mice in this study were reviewed by an externally established peer review panel, the Committee of the Ethics of the Research and Welfare of the Experimental Animals of the NIHS, and thereby approved by the Animal Care and Use Committee at the NIHS with the experimental code 224-37009639415-2002. Approved experiments were humanely performed in strict accordance with Guidelines for the Care and Use of Laboratory Animals, NIHS, Japan.

Blood and Bone Marrow Separation. Peripheral blood was collected from the orbital sinus. The numbers of peripheral white blood cells, platelets, and red blood cells were measured using a Coulter counter (Sysmex K-4500; Sysmex Co., Kobe, Japan). Bone marrow cells were harvested from the femur of each mouse (20) after animals were sacrificed by cervical dislocation under deep anesthesia with ethyl ether. A 26-gauge needle was inserted into the femoral bone cavity through the proximal and distal ends of the bone shafts, and bone marrow cells were flushed out under pressure by injecting 2 ml α-minimum essential medium (MEM) with ribonucleosides and deoxyribonucleosides (Invitrogen Corp., Carlsbad, CA). A single-cell suspension was obtained by gently and repeatedly drawing bone marrow cells through a 26-gauge needle and then a 27-gauge needle.

Antibodies. For immunobead-density gradient separation, the biotinylated antibody cocktail (BD Biosciences, San Jose, CA) containing anti-mouse CD3e (145–2C11), CD11b (M1/70), CD45R/B220 (RA3-6B2), Ly-6G and Ly-6C/Gr-1 (RB6-8C5), and TER-119/erythroid cell (TER-119) antibodies; and the monoclonal antibody cocktail SpinSep (StemCell Technologies Inc., Vancouver, BC, Canada) containing anti-CD5/Ly-1, CD45R, CD11b/Mac-1, Ly-6G/Gr-1, TER119, and 7/4/neutrophil antibodies were used as lineage (lin) markers. As a secondary antibody for the former biotinylated antibody cocktail, streptavidin–peridinin chlorophyll, a protein (PerCP; BD Biosciences) was used. For the latter cocktail, SpinSep, an optimized combination antibody cocktail against SpinSep that had been coated on dense microparticles, SpinSep Mouse Dense Particles (StemCell Technologies Inc.), was used for immunoprecipitation.

For immunomagnetic bead separation, CD117/c-kit

conjugated with phycoerythrin (PE; StemCell Technologies Inc.) was used as a progenitor marker, and an anti-PE tetrameric antibody complex (StemCell Technologies Inc.) was used as secondary antibody.

For flow cytometric analyses, the same antibody cocktails from BD Biosciences were used as lineage markers. In addition, a mouse anti-Cx32 monoclonal antibody from two sources (Chemicon International Inc., Temecula, CA, and Santa Cruz Technology Inc., Santa Cruz, CA) was used as the primary antibody for Cx32. As a secondary antibody, anti-mouse Ig conjugated with fluorescein isothiocyanate (FITC; BD Biosciences) was used.

For immunohistochemical analysis, the same anti-Cx32 antibody (Chemicon International, Inc.) was used as the primary antibody. As the secondary antibody, a biotinylated horse anti-mouse IgG antibody (Vector Laboratories Inc., Burlingame, CA) was used, and streptavidin labeled with peroxidase and 3,3′-diamino-benzidine (DAB) was used to detect immunoreactivity (Vector Laboratories Inc.).

Enrichment of Bone Marrow Cells in lin$^-$c-kit$^+$ Fraction. The lin$^-$c-kit$^+$ fraction is rich in hematopoietic stem cells (HSCs). To obtain a large number of lin$^-$c-kit$^+$-enriched fraction in the bone marrow cells, preseparation was carried out by the combination of immunobead density gradient and immunomagnetic bead separation. First, for the depletion of lineage-positive bone marrow cells, harvested bone marrow cells were processed through an immunobead density gradient using a density-matched medium and dense microparticles coated with a cocktail of an optimized combination of antibodies, SpinSep. Second, for selection of the c-kit$^+$ fraction, immunomagnetic bead separation using magnetic nanoparticles with a magnetic holder was carried out using the manufacturer's instruction (StemCell Technologies Inc.). For each procedure, the antibodies used are described in the subsection *Antibodies* in *Materials and Methods*.

Flow Cytometric Analysis Using Anti-Cx32 Antibody. Bone marrow cells with or without fractionation for lin$^-$c-kit$^+$ HSC enrichment were stained with the biotinylated antibody cocktail for streptavidin-PerCP, c-kit–PE, the anti-Cx32 antibody, and anti-mouse IgG conjugated with FITC. For exposure to the intracytoplasmic epitope of the anti-Cx32 antibody, cells were fixed with paraformaldehyde and then permeabilized with phosphate-buffered saline supplemented with HEPES and saponin (21). Flow cytometric analysis was carried out using FACS Vantage (BD Biosciences).

Irradiation. In the assay of hematopoietic progenitor cells, as well as in the repopulation bioassay for leukemogenesis (22), recipient mice were exposed to a lethal radiation dose of 915 cGy at a dose rate of 124 cGy/min using a ^{137}Cs-gamma irradiator (Gammacell 40 Exactor; MDS Nordin Inc., Ottawa, ON, Canada) with a 0.5-mm aluminum-copper filter.

Assay for Colony-Forming Units in Spleen (CFU-S). The Till and McCulloch method was used to determine the number of hematopoietic spleen colonies (CFU-Ss) (23) formed by hematopoietic progenitor cells. Aliquots of a bone marrow cell suspension were used for evaluating the number of CFU-Ss. Spleens were harvested 9 days after the bone marrow transplantation to determine the number of CFU-S-9 and 13 days to determine the number of CFU-S-13, and then were fixed in Bouin solution. Macroscopic spleen colonies were counted under an inverted microscope at magnification ×5.6. It was previously shown using the C57BL/6 strain that all colonies visible on Day 9 and Day 13 originate from the transplanted bone marrow cells under the condition that the recipient mice were exposed to a lethal radiation dose of 915 cGy (24).

Assay for Granulocyte-Macrophage Colony-Forming Units (CFU-GMs). CFU-GMs were assayed in semisolid methylcellulose culture (20, 24). Briefly, 8×10^4 bone marrow cells suspended in 100 μl α-MEM were added to 3.9 ml culture medium containing 1% methylcellulose (Nakarai-Tesque Co. Ltd., Kyoto, Japan), 30% fetal calf serum (HyClone Laboratories Inc., Logan, UT), 1% bovine serum albumin (Sigma, St. Louis, MO), 10^{-4} *M* mercaptoethanol (Sigma), and 10 ng/ml murine granulocyte macrophage colony-stimulating factor (GM-CSF; R&D Systems Inc., Minneapolis, MN). One-milliliter aliquots containing 2×10^4 cells were placed in 35-mm tissue culture wells (Nalgen Nunc International, Rochester, NY) in triplicate, and were incubated for 6 days in a fully humidified incubator at 37°C with 5% CO_2 in air. Colonies were counted using an inverted microscope at magnification ×40 (Olympus Optical Co. Ltd., Tokyo, Japan).

PCR Analysis for Genotyping. To detect Cx32 wild-type and Cx32-KO alleles, PCR analysis was performed using genomic DNA extracted from the tail of each mouse or from the hematopoietic tissues, spleen and bone marrow, or from tumor cells of the mice in the carcinogenesis tests, and synthetic oligonucleotides were used as primers (19). Hepatic tissues were assayed as the positive control materials (19). To detect the wild-type allele, the common 5′ primer (ccataagtcaggtgtaaaggagc) and the 3′ primer (agataagctgcagggaccatagg) were used; to detect the Cx32-KO allele, the common 5′ primer and *neo*-primer (atcatgcgaaacgatcctcatcc) were used.

Reverse Transcription (RT) and PCR Analysis of Cx32 Expression. The expression of the gene encoding Cx32 was analyzed by RT followed by PCR. The total RNA from the bone marrow cells and other tissues was isolated using a Qiagen RNAeasy kit (Qiagen, Valencia, CA). Since hepatocytes are known to express Cx32 (19), the liver was used not only as the hematopoietic organ, but also as the positive control in the verification by RT-PCR analysis. RT was performed using total RNA with random hexamers as primers, according to the instructions provided with the RT kit from Applied Biosystems (Foster City, CA). PCR amplification was performed using the following previously designed oligonucleotide primers including β-actin primers, an amplification control for RT-

PCR: Cx32-RT5, 5′-atgcacgtagcctcaccaacagcac-3′; Cx32-RT3, 5′-actcgtagccagcgagaaaagtcg-3′; murine β-actin-5′, 5′-gtaccacgggcattgtgatg-3′; and murine β-actin-3′, 5′-cgttctatcgtgtcgaagag-3′ (15).

Single-Dose Administration of MNU. Mice were randomly assigned to groups and individually housed. Immediately before use, MNU (Nakarai-Tesque Co. Ltd.) was dissolved in citrate buffer (0.01 *M* sodium citrate and 0.14 *M* NaCl, pH 5.5) and injected ip into the mice (25, 26).

Leukemogenicity Bioassay. Leukemogenicity was determined by a conventional whole-body bioassay and a transplantation bioassay (22). In the conventional whole-body assay, twelve 8-week-old Cx32-KO male mice ($Cx32^{-/Y}$) and ten wild-type littermates ($Cx32^{+/Y}$) were injected ip with MNU at 50 mg/kg body wt. In the transplantation bioassay, aliquots of single-cell suspension of the bone marrow (1×10^6 cells) from 8-week-old $Cx32^{-/Y}$ or $Cx32^{+/Y}$ male mice were injected into the tail vein of 8-week-old, 915-cGy–irradiated, wild-type female recipient mice. Only male mice were used as donors and only female mice were used as recipients to utilize the Y chromosome–specific sequence (a candidate testis-determining gene) for differentiating donor-derived neoplasms from recipient-derived neoplasms (27, 28). To study the effect of competitive repopulation on leukemogenicity, a group of mice was also injected with a mixture of cells, one half of which were Cx32-KO bone marrow cells and the other half wild-type bone marrow cells (mixture group). In this procedure, the numbers of CFU-S-9 transferred into each recipient mouse were 3.2 (wild type), 3.1 (mixture group), and 2.6 (Cx32-KO) $\times 10^2$. In this transplantation bioassay, bone marrow cells from Cx32-KO or wild-type mice were equally effective in protecting against the lethal dose of radiation, and bone marrow cellularity nearly reached that of the steady state after 4 weeks (data not shown). Four weeks after transplantation, 36 and 45 recipient mice were injected ip with MNU at 50 and 75 mg/kg body wt, respectively. The mice were supplied with water *ad libitum*. The mice in both the conventional leukemogenicity whole-body bioassay and in the transplantation bioassay were monitored throughout their lifetime at least twice daily. Those showing symptoms of advanced leukemia, such as anemia and palpable splenomegaly, were euthanized at the agonal period and then examined hematopathologically. Additionally, mice that died were subjected to gross and microscopic examinations (26).

Histopathological Examination. For the evaluation of hematopoietic malignancies caused by the injection of MNU in wild-type and Cx32-KO mice, mice from each group were sacrificed under ethyl ether anesthesia for necropsy. For the histopathological examination, all the visceral organs, including the thymus, spleen, sternum, and femoral bone marrow, were fixed in 4% neutral-buffered formalin for 24 hrs. The sternum and femoral bone marrow were decalcified in 7.5% formic acid for 72 hrs. After routine processing, paraffin-embedded sections were stained with hematoxylin and eosin and then examined histopathologically using a light microscope (22).

Immunohistochemical Staining. To confirm the cellular location of Cx32-positive progenitor cells, spleen colonies were examined by immunohistochemical staining with the anti-Cx32 antibody. Spleen sections containing colonies were fixed with 4% paraformaldehyde solution and embedded in paraffin for thin sectioning. The thin sections were then immunohistochemically stained with the anti-Cx32 antibody, a biotinylated secondary antibody, a horse anti-mouse IgG antibody, and streptavidin labeled with peroxidase to form the ABC complex with 3,3′-DAB.

Statistical Analyses. The data obtained were stored in a computer and processed for statistical analyses using the Kaplan-Meier method for survival curves and the log-rank test for their statistical significance. The Student *t*-test was used to evaluate the significance of differences in blood cell count, bone marrow cellularity, and the numbers of progenitor cells, CFU-GMs, CFU-S-9s, and CFU-S-13s between the wild-type group and the KO group. The incidence of hematopoietic neoplasms was evaluated by Fischer exact test. Differences with a P value <0.05 were considered significant.

Results

Expression of Cx32 in Hematopoietic Progenitor Cells and Its Function in Steady-State Hematopoiesis. *Expression of Cx32 in Hematopoietic Cells.* Figure 1A shows the expression of Cx32 in various lympho-hematopoietic tissues of wild-type mice. As previously reported (19), Cx32 was detected at the mRNA level only in the hepatic tissue by RT-PCR analysis, but was not detected in the spleen, bone marrow, and thymus.

Expression of Cx32 in Hematopoietic Spleen Colonies Developed from Progenitor Cells. We next studied Cx32 expression in colonies developed in the spleen of lethally irradiated wild-type recipient mice following injection of bone marrow cells from wild-type mice or Cx32-KO donor mice. Hematopoietic spleen colonies are rich in immature cells rather than in cells from peripheral blood or unfractionated bone marrow (24). As shown in Figure 1B, the expression of Cx32 detected by RT-PCR analysis was observed only in the hematopoietic spleen colonies but derived from wild-type bone marrow cells (a1 through a3), not in the colonies derived from Cx32-KO bone marrow cells (c1 and c2). Cx32 expression also was detected in the spleen colonies in Cx32-KO recipient mice repopulated with wild-type bone marrow cells (b1 and b2).

Immunohistochemical staining with the anti-Cx32 antibody was carried out to examine the hematopoietic spleen colonies originating from bone marrow cells from wild-type mice and Cx32-KO mice (Fig. 2). A colony originating from a wild-type bone marrow cell (Fig. 2Aa) shows mild and mottled staining in beige, whereas a colony originating from Cx32-KO bone marrow cells are negative

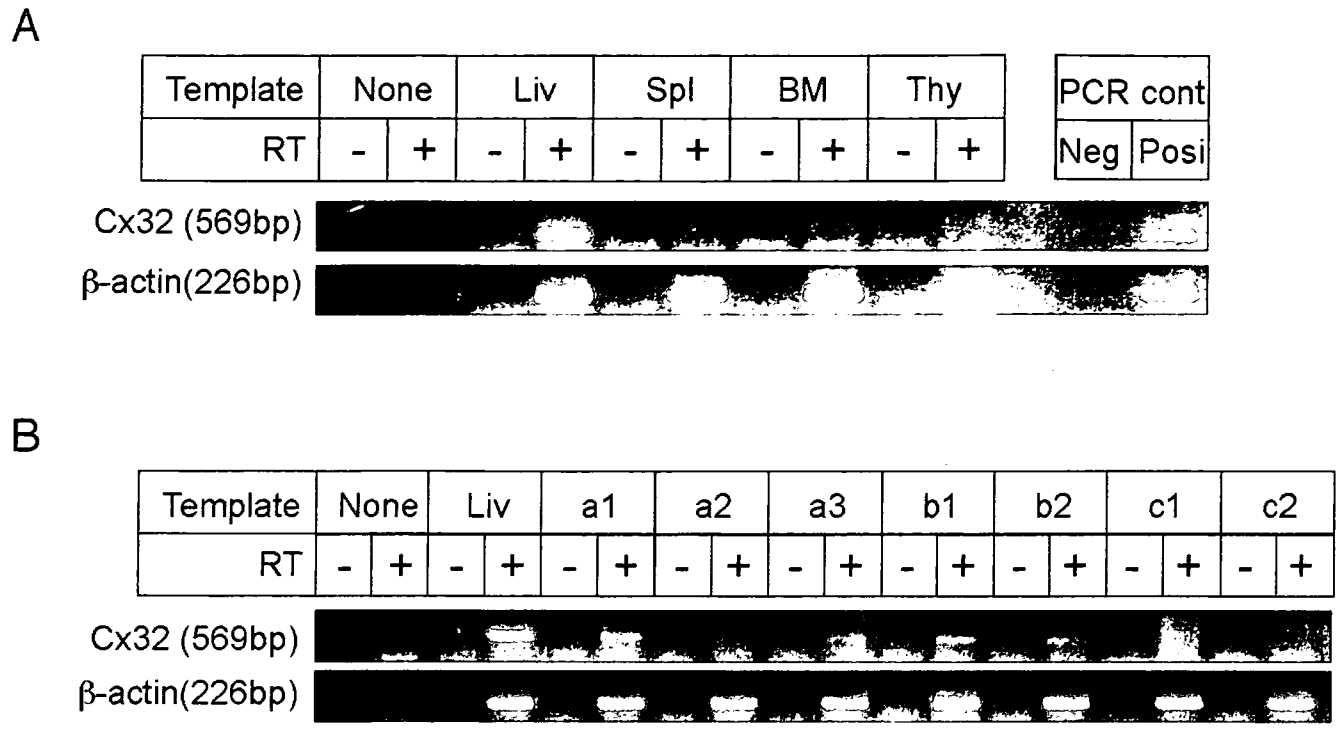

Figure 1. Expression of Cx32 in the lympho-hematopoietic tissues and hematopoietic spleen colonies. (A) Expression of Cx32 in lympho-hematopoietic tissues. Total RNAs were extracted for RT-PCR from the liver (Liv), spleen (Spl), bone marrow (BM), and thymus (Thy) of wild-type mice. Note that Cx32 expression was not detected in the spleen, bone marrow, or thymus, but was detected in the liver, a positive control (see *Materials and Methods*). PCR: for "Neg" lane and "Posi" lane, no template and whole genome extracted from the tail were loaded, respectively. RT(+) and RT(–): With or without Avian reverse transcriptase, 2.5 U/20 μl, respectively (see *Materials and Methods*). (B) Expression of Cx32 in hematopoietic spleen colonies (see *Materials and Methods*). Lethally irradiated wild-type mice were injected with bone marrow cells from wild-type or Cx32-KO donor mice. After 9 days, total RNAs extracted from individual hematopoietic spleen colonies derived from wild-type bone marrow cells or those from Cx32-KO bone marrow cells were reverse transcribed followed by PCR and then loaded (a1–a3, c1 and c2). Total RNAs extracted from colonies derived from wild-type bone marrow cells removed from the lethally irradiated Cx32-KO recipient mice followed by repopulation with wild-type bone marrow cells were similarly loaded (b1 and b2).

in staining (Fig. 2Ba and b). Interestingly, in a colony observed at a higher magnification (Fig. 2Ab), cells from wild-type mice positively stained by the anti-Cx32 antibody were only scattered in the outer boundary of spleen colonies (circled by dotted line in Fig. 2Aa and arrows in Fig. 2Ab), indicating that the incidence of primitive progenitor cells was still low in the spleen colonies.

Expression of Cx32 in Hematopoietic Stem Cell Compartment. We then next determined whether Cx32-positive cells are consistently found in the HSC compartment. First, the $lin^-c\text{-}kit^+$ HSC-enriched fraction was obtained by the combination of immunobead-density gradient separation for depleting lineage-positive cells and immunomagnetic bead separation for selecting $c\text{-}kit^+$ cells, followed by flow cytometric analysis using the anti-Cx32 antibody. As a result, the separated $lin^-c\text{-}kit^+$ HSC fraction was 0.25% with respect to the original unfractionated wild-type bone marrow cells. Figure 3 shows the flow cytometric distribution of the $lin^-c\text{-}kit^+$ HSC-enriched fraction (Fig. 3B) compared with original unfractionated cells (Fig. 3A) from both wild-type bone marrow cells (the horizontal axis for lineage markers and the vertical axis for c-kit). In Figure 3B, the percentage of $lin^-c\text{-}kit^+$ compartment (HSC compartment) indicated by an asterisk is 90.2% of the $lin^-c\text{-}kit^+$ HSC-enriched preseparated fraction. Furthermore, the number for $lin^-c\text{-}kit^+$ compartment (asterisk in Fig. 3B) is 106.9 times enriched compared to the fraction of the original unfractionated bone marrow cells, as shown in the enclosed corresponding square (Fig. 3A). To determine which fraction Cx32-positive cells belong to, bone marrow cells from wild-type mice and Cx32-KO mice were stained with lineage-PerCP, c-kit–PE, and Cx32-FITC with or without the $lin^-c\text{-}kit^+$ HSC enrichment. In Figure 3C, 28.8% of the $lin^-c\text{-}kit^+$ fraction of wild-type bone marrow cells was found to be Cx32 positive (unshaded profile) compared with the same fraction of bone marrow cells obtained from Cx32-KO mice (shaded profile), which was used as the negative control. Together with frequency data of the $lin^-c\text{-}kit^+$ HSC-enriched fraction, Cx32-positive cells are calculated nearly 0.27% with respect to the original unfractionated whole bone marrow cells.

Whether the mature cell fraction, a $lin^+c\text{-}kit^-$ fraction, contains Cx32-positive cells, the fraction of wild-type bone marrow cells (unshaded profile) is compared to that of the control profile from Cx32-KO mice (shaded profile), as shown in Figure 3D. Since both fractions are nearly identical, few cells may be positive for Cx32 in the $lin^+c\text{-}kit^-$ fraction (0.27% of the $lin^+c\text{-}kit^-$ fraction; Fig. 3D).

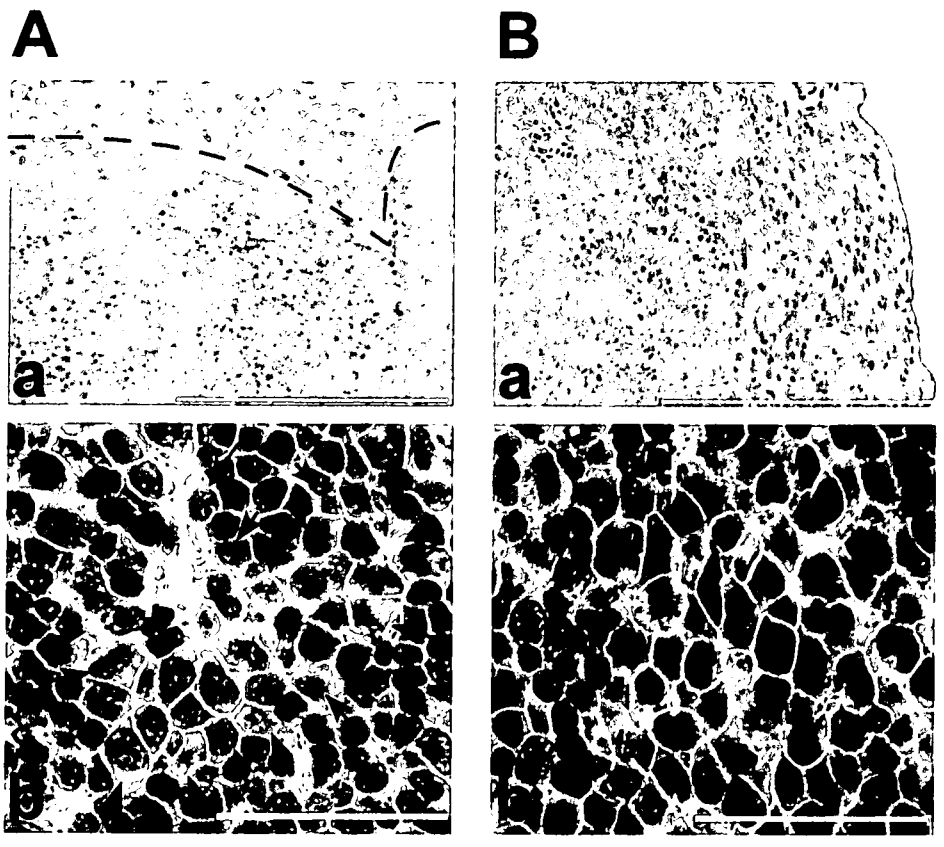

Figure 2. Cells in spleen colonies immunohistochemically stained with anti-Cx32 antibody. (A) Spleen colonies derived from wild-type bone marrow cells (a and b). (B) Cx32-KO bone marrow cells (i.e., control for negative staining; subpanels a and b). As shown in Aa and Ba, cells from spleen colonies were found positively stained with a mottled pattern in the former figure and negatively stained in the latter figure. The positively stained cells are located only in the outer boundary of the colony. Dotted line in Aa indicates border of the colony. Ab and Bb show a higher magnification of spleen colonies derived from wild-type mice and Cx32-KO mice, respectively. As shown in Ab, a colony was a mottled pattern with positively stained cells (arrows) in beige. Bb shows the negative control. Spleens were stained with the anti-Cx32 antibody and with the biotinylated secondary antibody, horse anti-mouse IgG antibody, and streptavidin labeled with peroxidase. Bars indicate 200 μm in Aa and Ba, and 25 μm in Ab and Bb.

Cx32-positive cells are 0.0093% with respect to the original unfractionated whole–bone marrow cells (data not shown).

Function of Cx32 in the Steady-State Hematopoiesis. The steady-state hematopoiesis of wild-type mice was compared to that of Cx32-KO mice. Figure 4A shows the comparison of the absolute body weight, splenic weight, and cellularity of the bone marrow. There were essentially no differences in any of these parameters between wild-type mice and Cx32-KO mice. However, the number of white blood cells and that of platelets were significantly different between wild-type mice and Cx32-KO mice, as shown in Figure 4B. Regarding the decrease in the number of white blood cells, there was no trend toward decrease between numbers of lymphocytes and neutrophils. Moreover, there was no difference in the number of red blood cells. Regarding the number of CFU-GMs, there was a significantly lower number of progenitor cells per unit number of bone marrow cells in Cx32-KO mice than in wild-type mice. Hematopoietic progenitor cells that form CFU-S-9s are considered to be more mature than those that form CFU-S-13s (29, 30). As shown in Figure 4C, in terms of the maturation stages from CFU-S-13 and CFU-S-9 to CFU-GM, the number of all of the hematopoietic progenitor cell compartments of Cx32-KO mice was lower than that of the wild-type mice. Therefore, the present study clearly showed that Cx32 deficiency induced an impaired hematopoiesis specifically in the immature progenitor cell fraction, and changes in differentiated cells may be a reflection of those in immature cells. Thus, Cx32 is assumed to be required for the maintenance of immature hematopoietic progenitor cells.

Function of Cx32 During Growth of Hematopoietic Progenitor Cells. Although the stromal cell–dependent connexin Cx43 is known to function in cultured stromal cells (12, 13), few cells were positive in anti-Cx32 antibody in the bone marrow. Thus, one question is to answer is whether the hematopoietic defect observed in Cx32-KO mice exists solely in hematopoietic progenitor cells, or also in stromal cells. Accordingly, to examine whether Cx32 deficiency has a negative effect on hematopoiesis in stromal cells of Cx32-KO mice, lethally irradiated wild-type mice and Cx32-KO mice were repopulated with bone marrow cells from wild-type mice or Cx32-KO mice. Results from four different combinations are shown in Figure 5.

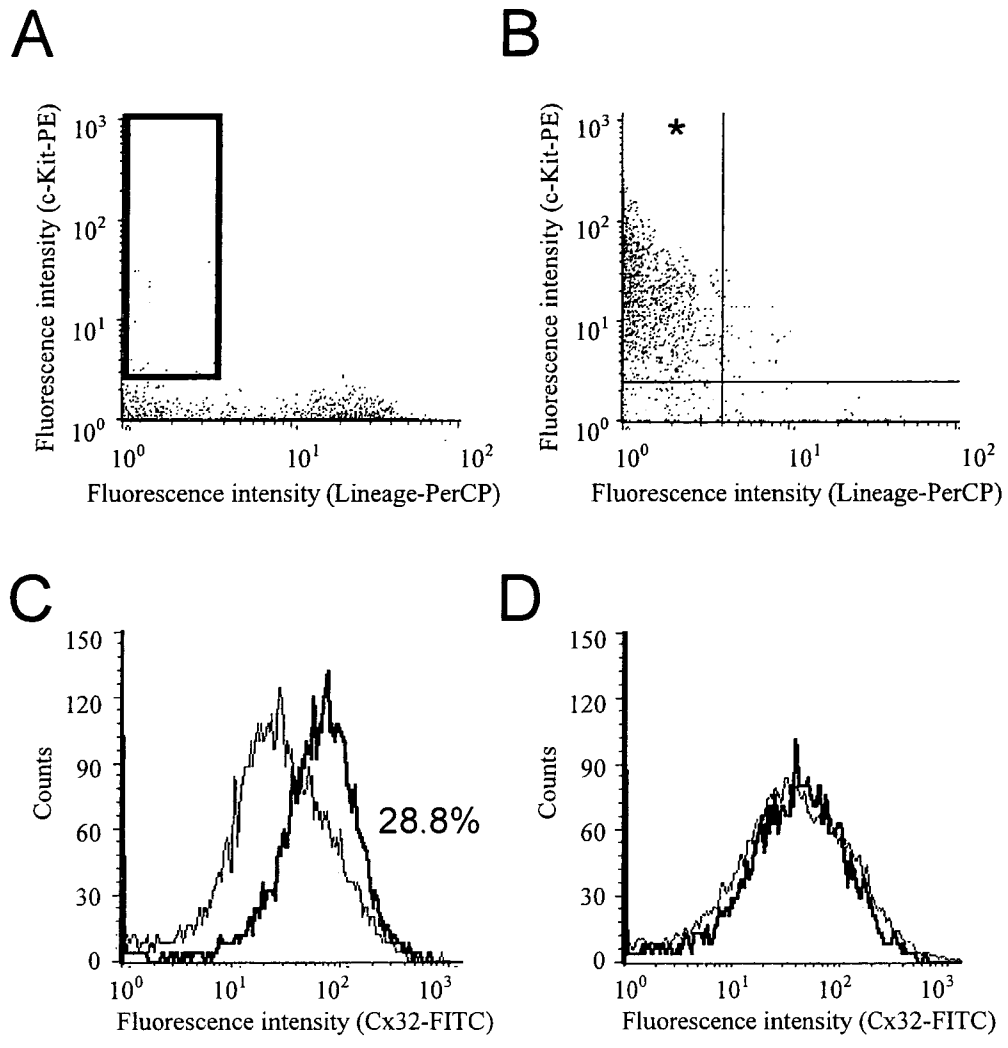

Figure 3. Flow cytometric analyses for lin$^-$c-kit$^+$ HSC-enriched fraction and lin$^-$c-kit$^+$ Cx32-positive cells from wild-type mice. Flow cytometry after bone marrow cell separation carried out by a combination of the immunobead-density gradient separation and the immunomagnetic bead separation. (A) Unseparated bone marrow cells. (B) Bone marrow cells fractionated by combination of the immunobead-density gradient separation for eliminating lineage marker positive cells and the immunomagnetic bead separation for c-kit$^+$ cells. The vertical axis in both figures indicates fluorescence intensity for the PE-labeled anti–c-kit antibody, and the horizontal axis indicates fluorescence intensity for Per-CP–labeled streptavidin for biotinylated lineage antibodies. The vertical and horizontal lines in panel B indicate the negative and positive borders of fluorescence intensity. The asterisk in panel B indicates the targeted lin$^-$c-kit$^+$ compartment and HSC compartment. Note that the corresponding area of the asterisk in panel B is indicated by the square box in panel A. (C and D) Histogram of the FITC-labeled anti-Cx32 antibody. The lin$^-$c-kit$^+$ fraction (C) and the lin$^+$c-kit$^-$ fraction (D) for wild-type bone marrow cells (open profile with bold line) and the same fraction for Cx32-KO bone marrow cells (shaded profile), a negative control. Cx32-positive fraction in panel C calculated for the lin$^-$c-kit$^+$ fraction in wild-type bone marrow cells is 28.8%.

Regardless of the expression of Cx32 in stromal cells in either Cx32-KO recipient mice or wild-type recipient mice, there were no statistically significant differences in the number of spleen colonies (CFU-S-9s) between the pair of groups that received either wild-type bone marrow cells (Fig. 5A, two left columns) or Cx32-KO bone marrow cells (Fig. 5A, two right columns). Thus, Cx32 deficiency in progenitor cells is concluded as a major factor that is responsible for the production of a significantly small number of colonies. As observed in Figure 4C, it is confirmed that the number of colonies is larger when donor bone marrow cells are from wild-type mice than when they are from Cx32-KO mice.

In Figure 5B, the size of spleen colonies in each group is shown. Significantly smaller colonies were observed in the three groups in which recipient mice, donor bone marrow cells, or both were from Cx32-KO mice rather than in the group in which both recipient mice and donor bone marrow cells were from wild-type mice (Fig. 5B, open column). Because there was no significant difference in size between groups repopulated with Cx32-KO bone marrow cells, the major factor for producing small colonies (Fig. 5B, two right columns) also is assumed to be responsible for Cx32 deficiency in donor progenitor cells, rather than any factor from stromal cells. Concerning the group that received wild-type bone marrow cells (Fig. 5B, the second